AD 406 417

406417

JPRS: 17,398

31 January 1963

S&T

Scale-1

406 417

AD No. FILE COPY

THE ZEEMAN PHENOMENON AND MAGNETIC RESONANCE

by M. A. Yel'yashevich

- USSR -

U. S. DEPARTMENT OF COMMERCE
OFFICE OF TECHNICAL SERVICES
JOINT PUBLICATIONS RESEARCH SERVICE
Building T-30
Ohio Dr. and Independence Ave., S.W.
Washington 25, D. C.

Price: $2.00

FOREWORD

This publication was prepared under contract for the Joint Publications Research Service, an organization established to service the translation and foreign-language research needs of the various federal government departments.

The contents of this material in no way represent the policies, views, or attitudes of the U. S. Government, or of the parties to any distribution arrangements.

PROCUREMENT OF JPRS REPORTS

All JPRS reports are listed in Monthly Catalog of U. S. Government Publications, available for $4.50 ($6.00 foreign) per year (including an annual index) from the Superintendent of Documents, U. S. Government Printing Office, Washington 25, D. C.

Scientific and technical reports may be obtained from: Sales and Distribution Section, Office of Technical Services, Washington 25, D. C. These reports and their prices are listed in the Office of Technical Services semimonthly publication, Technical Translations, available at $12.00 per year from the Superintendent of Documents, U. S. Government Printing Office, Washington 25, D. C.

Photocopies of any JPRS report are available (price upon request) from: Photoduplication Service, Library of Congress, Washington 25, D. C.

THE ZEEMAN PHENOMENON AND MAGNETIC RESONANCE

- USSR -

[Following is the translation of Chapter 14 of the Russian-language book by M. A. Yel'yashevich, Atomnaya i molekulyarnaya spektroskopiya (Atomic and Molecular Spectroscopy), Moscow, 1962, State Publishing House for Physico-Mathematical Literature, pages 367-408.]

14.1 Splitting of Energy Levels in a Magnetic Field

In a magnetic field degenerated levels of energy of the atom are separated into nondegenerate sublevels. This results in magnetic cleavage of the spectral lines corresponding to the transition between various energy levels into many component levels, and to the appearance of forced transitions between sublevels of a given level of energy.

The phenomenon of cleavage of spectral lines and energy levels in a magnetic field is called the Zeeman phenomenon. Zeeman first discovered (in 1896; cf. Paragraph 1.6, page 34) dilation of the Na 5890-5896 A doublet line (first member of the main series, cf., for example, page 224) in a magnetic field; later he observed not only dilation, but also cleavage of spectral lines. Lorentz explained this on the basis of the classic electron theory as the result of cleavage of the frequency of vibration of an elastically bound electron of the atom, and it was not until later that it was interpreted in its natural form, on the basis of the Bohr theory, as the result of cleavage of energy levels. At present the term "Zeeman phenomenon" is applied to the splitting of both spectral lines and energy levels in a magnetic field (which already has been mentioned in Paragraph 1.5, page 31). Study of the Zeeman phenomenon, or effect, in the spectral lines of atoms in both the visible and ultraviolet range played a great role in the development of the science of atomic structure, particularly in the period following the development of the Bohr theory. At the present time investigation of the Zeeman effect in spectral lines of atoms is one of the most important methods of determining the characteristics of the energy levels of atoms and greatly facilitates interpretation of complex atomic spectra; study of the Zeeman splitting of spectral lines also enables acquisition of valuable data on magnetic fields in light sources, particularly in study of the Sun, its magnetic fields and sun spots.

Forced transitions between Zeeman sublevels of a given energy level occur under the effect of irradiation of a frequency equal to the frequency of the possible transitions, i.e., in the case of resonance, and this phenomenon is called the magnetic resonance. The frequencies of transitions between Zeeman sublevels lie in the radiofrequency range of the spectrum and are studied by radiospectroscopic methods (40, 41). Magnetic resonance first was discovered in 1938 by Rabi and his associates (243) in molecular beams*. He first discovered resonance transitions between sublevels of Zeeman splitting for the hydrogen molecule, caused by the magnetic moments of the proton and deuteron, and then in 1940 (244) he observed transitions between sublevels of Zeeman splitting in atoms, caused by electron magnetic moments of atoms. The study of magnetic resonance, both electronic and nuclear, in atomic and molecular beams is very complex in its experimental methodology, and investigation of this phenomenon began to expand only after the discovery by Zavoyskiy in 1944 in Kazan (245) of electronic paramagnetic resonance, absorption of microwave irradiation by a substance due to transitions between sublevels of Zeeman splitting connected with the electron magnetic moments of particles of the substance (determined by the paramagnetic properties of the substance, hence the name "paramagnetic" resonance); an analogous phenomenon of ferromagnetic resonance** is observed in ferromagnetic substances. Nuclear paramagnetic resonance, or absorption of irradiation in the range of short radio waves with Zeeman splitting in a substance was observed by US investigators (246). This was due to nuclear magnetic moments. Paramagnetism connected with nuclear magnetic moments was discovered by Lazarev and Shubnikov in 1937 (242) in the course of investigation of the magnetic properties of solid hydrogen at a temperature of 2 to 4° K. At the present time the majority of the great number of radiospectroscopic investigations being conducted are performed with the aid of various methods of magnetic resonance. Essentially, these methods enable determination of the magnetic moments of atoms and nuclei with a very high degree of precision (cf. page 401).

---

*) Directed beams of neutral particles are called molecular beams. They are subdivided into actual molecular beams consisting of molecules, and atomic beams, consisting of atoms.

**) The first experiments on ferromagnetic resonance were performed by Arkad'yev in 1926 (36), although the general theory was developed in 1935 by Landau and Lifshits (241). Numerous experimental investigations of ferromagnetic resonance have been conducted since 1946.

In the following we present a detailed discussion of the Zeeman splitting of spectral lines (Paragraphs 14.2 to 14.5) and magnetic resonance (Paragraphs 14.6 to 14.8); in the present paragraph we discuss the Zeeman splitting of energy levels as the basis of further discussions.

According to graphic representation, the cause of Zeeman splitting of energy levels is the fact that magnetic moments may be oriented by various means in relation to the magnetic pole.

Additional energy in the magnetic field of any atomic system having magnetic moment depends upon the orientation of the moment in question in relation to the field, specifically the magnitude of projection of this moment upon the direction of the field. The projection μ_z of the magnetic moment μ is proportionate to the projection J_z of the mechanical moment J, and is quantized together with it (cf. Paragraph 2.5, page 51). As a result, to each value of projection of the moment of quantity of motion corresponds a definite value of the projection of the magnetic moment and its value of supplementary energy in the magnetic field. In conformance with $2J+1$ possible values $m_J = m = J, J-1, \ldots, -J$ projections of J_z of the mechanical moment J multiplicity of disintegration is equal to $g_J = 2J+1$, and determines the number of sublevels in the magnetic field (cf. Paragraph 2.12 and Paragraph 2.15). The quantum number m, characterizing the sublevel of Zeeman splitting, has received the name magnetic quantum number (cf. page 50).

Let us examine in greater detail the splitting of the energy level of an atom having electron magnetic moment μ_e, in a constant external magnetic field of intensity H.

According to the known formula for the energy of a magnet located in a magnetic field, the excess energy of the atom is equal to:

$$\Delta E = -(\mu H) = -\mu H \cos(\mu, H) = -\mu_z H, \qquad (14.1)$$

where $\mu_z = \mu \cos(\mu, H)$ is the projection of the magnetic moment in the direction of the field along the z axis, and in the case under consideration is the isolated direction which we previously

had selected for the z axis. In distinction from the case of a free system, for which any given direction of the axis of quantization may be selected, we now have a physically isolated direction of the magnetic field.

The projection μ_z of magnetic moment in the direction of the of the field has a definite value (2.43), and we obtain

$$\Delta E_m = -\gamma \hbar m H, \qquad (14.2)$$

where γ is the gyromagnetic (magnetomechanical) relationship and $m = m_j$ acquires the value of $2J+1$. The formula (14.2) gives the splitting of the original level into 2J+1 equidistant sublevels, as is indicated in Figure 14.1, for the least integral and semi-integral values of J. The initial position of the level prior to its splitting is indicated by the broken line. Splitting is symmetrical with respect to this position, which at an integral J coincides with the position m = 0 of the sublevel. The distance between neighboring sublevels is equal to $\gamma \hbar H$, i.e., is proportionate to the gyromagnetic ratio and the intensity of the magnetic field.

For a purely orbital moment the gyromagnetic ratio is determined by formula (2.45), and formula (14.2) assumes the form

$$\Delta E_m = -\gamma_l \hbar H m = \frac{e\hbar}{2m_e c} H m = \mu_B H m, \qquad (14.3)$$

where μ_B is the magneton of Bohr (2.46). The sublevels with subsequent values of m are located at distances $\mu_B H$. In the same way that the magneton of Bohr is a natural unit for measurement of electron magnetic moments, the value $\mu_B H$ is a natural unit for measurement of the splitting of atomic energy levels in a magnetic field. It gives the magnitude of splitting for purely orbital moment, and often is called the magnitude of normal splitting.

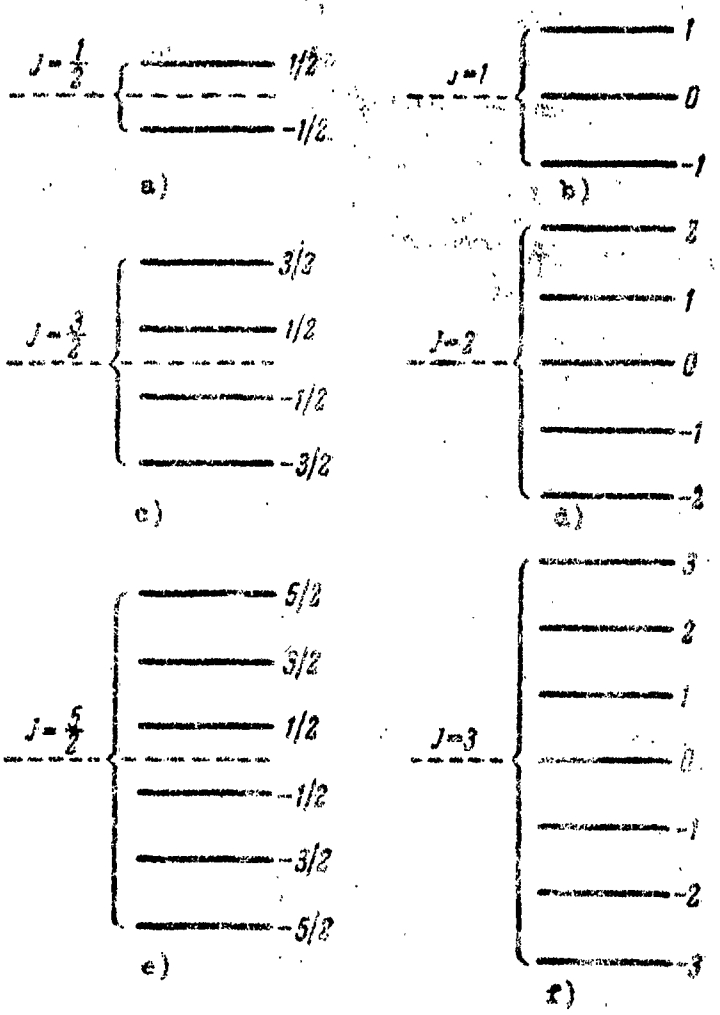

Figure 14.1. Splitting of levels in a magnetic field with various values of J:

a) - at J = 1/2;
b) - at J = 1;
c) - at J = 3/2;
d) - at J = 2;
e) - at J = 5/2;
f) - at J = 3.

For a purely spin moment we obtain, according to formula (2.55)

$$\Delta E_m = -\gamma_s \hbar H m = \frac{e\hbar}{m_e c} H m = 2\mu_B H m. \qquad (14.4)$$

The distance between adjacent sublevels is equal to $2\mu_B H$, i.e., twice the value of normal splitting. In the very important case of of an electron with noncompensated spin, at

$$l = 0,\ m = m_s = \pm 1/2 \text{ (cf. (6.6))},$$

and an initial level with value $j = s = 1/2$ splits into two half-levels (cf. Figure 14.1 a), located at distance $2\mu_B H$. It may be noted that for both orbital and spin moment the sublevel with the least m (cf. (14.3) and (14.4)) lies deepest, because of the negative value of γ (due to negative electron charge).

Let us evaluate at this point the value of normal splitting $\mu_B H$. According to (2.47) the numerical value of the magneton of Bohr is equal to

$$\mu_B = 0{,}92731 \cdot 10^{-20} \frac{\text{erg}}{\text{gauss}} \approx 1{,}400 \cdot 10^{6} \frac{\text{sec}^{-1}}{\text{gauss}} \approx 4{,}67 \cdot 10^{-5} \frac{\text{cm}^{-1}}{\text{gauss}}. \qquad (14.5)$$

In a magnetic field with 1 gauss intensity the Zeeman split $\mu_B H$ is equal to $4.67 \cdot 10^{-5}$ cm^{-1}, i.e., approximately $\frac{1}{20{,}000}$ cm^{-1}. In a magnetic field H = 20,000 gauss we have

$$\mu_B H = 0{,}934\ \text{см}^{-1} \approx 1\ \text{см}^{-1}\ (H = 20\,000\ \text{gauss}). \qquad (14.6)$$

Thus the value of normal splitting in a 20,000-gauss field is on the order of 1 cm^{-1}. In very strong permanent magnetic fields on the order of 100,000 gauss, which are applied in practice for study of the Zeeman effect, $\mu_B H$ is approximately 5 cm^{-1}*. Because of this

---

*) Fields of this type were applied by Harrison and Bitter (240); stronger fields were obtained by Kapitsa, Strelkov and Laurman (239).

the relative splitting of spectral lines in the visible and ultraviolet ranges (wave numbers on the order of several tens of thousands cm^{-1}) is low, even in very strong magnetic fields.

In studying electronic magnetic resonance magnetic fields not exceeding 5,000 to 10,000 gauss are used. In a field in which H = 5,000 gauss, $\mu_B H = 0.233\ cm^{-1}$/gauss, which corresponds to the wave length λ of resonant transition between adjacent sublevels of approximately 4.3 cm, and relating to the microwave region of the spectrum.

For an arbitrary electronic moment of an atom, we have, according to (14.2) and 14.3):

$$\Delta E_m = -\frac{\gamma}{\gamma_l}\gamma_l h H m = \frac{\gamma}{\gamma_l}\mu_B H m. \qquad (14.7)$$

Introducing the factor $g = \frac{\gamma}{\gamma_l}$, (14.7) may be written as:

$$\Delta E_m = g\mu_B H m \qquad (m = J, J-1, \ldots, -J). \qquad (14.8)$$

The factor g (Lande factor) determines the ratio of the relative magnitude of splitting $g\mu_B H$ for an arbitrary magnetic moment to the value of normal splitting $\mu_B H$. For purely orbital moment, g = 1, and for purely spin moment, g = 2. For electronic moment comprising the sum of orbital and spin moments g may have various values, from fractions of a unit to several units, depending upon the number of component moments and upon the type of relationship. The value of the factor g is an important characteristic of the energy level (cf. in detail Paragraph 14.3, below).

Formula (14.8) leads to a linear function of the Zeeman splitting in respect to the intensity of the magnetic field H. This is illustrated by the diagrams of Figure 14.2, in which the sublevel energy is represented the function of H for the values J = 1/2, 1, 3/2 and 2. This type of diagram is very useful for all cases in which the splitting of energy level is studied at various values of magnetic field, and especially in divergence from a linear relationship.

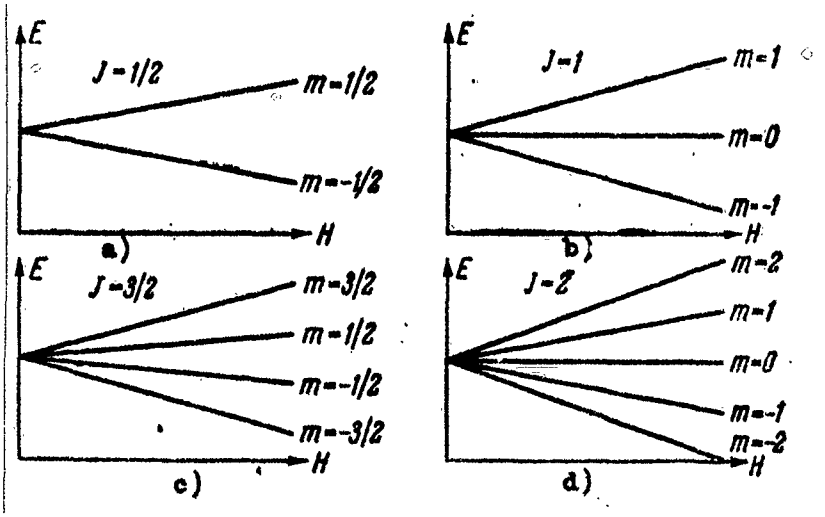

Figure 14.2. Splitting as a function of intensity of magnetic field:

a) - at J = 1/2; c) - at J = 3/2;
b) - at J = 1; d) - at J = 2

The linear function, determined by the main formula (14.8) for Zeeman splitting, holds only for an individual energy level E_i, far removed for other values of E_j. "Far removed" means that (considering g on the order of unity) the distance to adjacent levels is much greater than the value $|\mu_B H$.

$$|\mu_B H \ll |E_i - E_j|. \qquad (14.9)$$

A field satisfying the condition (14.9) is called a weak field, and thus formula (14.8) determines Zeeman splitting in a weak field. In distinction from (14.9) a field for which the converse condition

$$|\mu_B H \gg |E_i - E_j|, \qquad (14.10)$$

is fulfilled is called a strong field. The cases of strong fields and fields intermediate between strong and weak, when $|\mu_B H \sim |E_i - E_j|$, will be discussed below (cf. Paragraph 14.5).

It is apparent that the concepts of weak and strong fields are relative concepts, because they depend upon the amount of distance between adjacent energy levels in the absence of a magnetic field.

Starting out from formula (14.2) for supplementary energy in a magnetic field, we obtain the quantum mechanical energy by converting from the classic expression for supplementary energy $\Delta E = V = -\mu_z H$ of an atom with magnetic moment μ (cf. (14.1)), to the operator

$$\hat{V} = -H\hat{\mu}_z \tag{14.11}$$

and consider $\hat{V}$ as disturbance.

In the first approximation of the theory of disturbance, the supplementary energy is equal to the average value of the operator $\hat{V}$:

$$\Delta_1 E_{\alpha Jm} = \bar{\hat{V}} = V_{\alpha Jm,\,\alpha Jm} = \int \psi^*_{\alpha Jm} \hat{V} \psi_{\alpha Jm}\, dx$$

$$= -H \int \psi^*_{\alpha Jm} \hat{\mu}_z \psi_{\alpha Jm}\, dx = -H\bar{\hat{\mu}}_z, \tag{14.12}$$

taken according to the function of zero approximation $\psi_{\alpha Jm}$ (where α includes the characteristics of position apart from J and m). The average value of the operator of the projection of the magnetic moment is proportionate to the average value of the operator $\hat{M}_{pz} = \hbar \hat{J}_z$ of the projection of the mechanical moment, and may be expressed in the form

$$\bar{\hat{\mu}}_z = \int \psi^*_{\alpha Jm} \hat{\mu}_z \psi_{\alpha Jm}\, dx = \gamma\hbar \int \psi^*_{\alpha Jm} \hat{J}_z \psi_{\alpha Jm}\, dx =$$

$$-g\mu_B \int \psi^*_{\alpha Jm} \hat{J}_z \psi_{\alpha Jm}\, dx, \tag{14.13}$$

where γ is the relationship of magnetic, to mechanical moment, introduced in Chapter 2, and which for electronic moments may be expressed in Bohr magnetons μ_B and the factor $g\left(\gamma\hbar = \frac{\gamma}{\gamma_l}\gamma_l\hbar = -g\mu_B \text{ см. (14.7)}\right)$.

Considering that according to (2.19) and (2.10)

$$\hat{J}_z \psi_{\alpha Jm} = m\psi_{\alpha Jm} \qquad (m = m_J = J,\ J-1, \ldots, -J) \tag{14.14}$$

and, therefore, $\int \psi^*_{\alpha Jm} \hat{J}_z \psi_{\alpha Jm}\, dx = m$, we find

$$\bar{\hat{\mu}}_z = \gamma\hbar m = -g\mu_B m. \tag{14.15}$$

whence we obtain

$$\Delta_1 E = \Delta E_m = -\gamma\hbar H m = g\mu_B H m, \qquad (14.16)$$

i.e., formulas (14.2) and 14.8).

It appears that we had applied quantum mechanics earlier in unclear form when we inserted the quantum value μ_z according to (2.43) in the classic formula (14.1).

From the conclusion above it follows that the result (14.2) is correct only in the first approximation of the theory of disturbance. In the second approximation of the theory of disturbance the energy correction is determined by the non-diagonal matrix elements

$V_{\alpha Jm,\ \alpha' J' m}$ of the energy of disturbance, connecting position with the same value m and with values of J,, differing by no more than the value $(J' - J = \pm 1, 0)$. . This correction is equal to

$$\Delta_2 E = \sum \frac{|V_{\alpha Jm,\ \alpha' J' m}|^2}{E_J - E_{J'}} \qquad (\alpha' \neq \alpha,\ J' = J,\ J \pm 1), \qquad (14.17)$$

where summation is performed for all levels $\alpha' J'$, for which J' is distinguished from J by no more than unity. Because the matrix elements $V_{\alpha Jm,\ \alpha' J' m}$ are proportionate, as in the case of the matrix elements of (14.12), and the field intensity is H, then $\Delta_2 E$ is proportionate to H^2, which leads to the quadratic Zeeman effect. The relationship of the magnitude of the quadratic Zeeman effect to the value of the linear effect is on the order of:

$$s \approx \frac{|V_{\alpha Jm,\ \alpha' J' m}|}{|E_J - E_{J'}|}, \qquad (14.18)$$

i.e., the ratio of the matrix elements of the energy of disturbance to the difference in energy of adjacent levels. Because the matrix elements have the order $\mu_B H$ for electronic moments, the ratio (14.18) will be on the order of

$$s = \frac{\mu_B H}{|E_J - E_{J'}|}. \qquad (14.19)$$

If the given ratio ceases to be small, this means that the magnetic field is not weak, and splitting of the given level of energy may not be considered independently of splitting of other levels. We obtain a foundation for (14.9) as a criterion of the applicability of formula (14.2).

In closing the present paragraph we may mention that formulas (14.1) and (14.2) are general, and may be applied not only to atoms, but also to any given particles, both more complex, which are molecules, and simpler, which are elementary particles, specifically electrons, protons and neutrons. Formulas (14.8) through (14.10) are correct for any electronic magnetic moments, but analogous formulas are used for nuclear and rotational moments, distinguished only by replacement of the Bohr magneton μ_B by the nuclear magneton μ_{nuc} (cf. Paragraph 2.5), resulting in reduction of all scales by the function $\frac{\mu_B}{\mu_{nuc}} = \frac{m_p}{m_e}$.

14.2 General View of Zeeman Splitting of Spectral Lines in a Weak Field

The picture of Zeeman splitting of a given spectral line is determined by splitting of the combining levels and by correct selection for the magnetic quantum number. This, which according to (4.157) is correct for dipolar radiation, has the form

$$\Delta m = m_1 - m_2 = 0, \pm 1, \qquad (14.20)$$

where m_1 and m_2 are the magnetic quantum numbers of the combining levels. Therefore, upon conversion, the projection $J_z = m$ of mechanical moment (expressed in the units $\hbar = \frac{h}{2\pi}$) either remains unchanged, or changes by ± 1.

In conformance with the rules of selection (14.20), in conversions between sublevels of two combined levels, two types of components are obtained: π-- components, for which $\Delta m = m_1 - m_2 = 0$ and σ-- components, for which $\Delta m = m_1 - m_2 = \pm 1$. The possible conversions between the sublevel levels $J_1 = 3$ and $J_2 = 2$ are shown in Figure 14.3. The group of π-- components corresponds to the conversion $m \rightarrow m$ $(m_1 = m_2)$, the left group of σ-- components corresponds to the conversion $m - 1 \rightarrow m$ $(m_1 - m_2 = -1)$, and the right group of σ-- components corresponds to the conversion $m + 1 \rightarrow m$ $(m_1 - m_2 = 1)$.

The group of π-- components $(\Delta m = 0)$ and two groups of σ-- components $(\Delta m = -1, \Delta m = +1)$ are distinguished by polarization. The π-- components (parallel components) correspond to linear vibrations of the radiating dipole parallel to the direction of the field z, the σ-- components (perpendicular components)

correspond to circular vibrations of the radiating dipole in the plane xy perpendicular to the direction of the field, as is shown in the lower portion of Figure 14.2. In this, for $\Delta m = +1$ the direction of rotation is connected with the direction of the magnetic field in clockwise direction, and for $\Delta m = -1$ in counterclockwise direction.

The plarization of the Zeeman components derives from the relationships of (4.172) for the components of the vector which were developed in Paragraph 4.8. The rule of selection $\Delta m = 0$ corresponds to a linear oscillator oriented along the z axis, and the rule of selection $\Delta m = \pm 1$ corresponds to two linear oscillators oriented along the x and y axes, oscillating with a phase difference of $\pm \frac{\pi}{2}$, which gives a circular vibration. For dipolar radiation we have ordinary electrical oscillators which from the classic point of view comprise electrons describing harmonic vibration with acceleration $a = -\omega^2 r$, where $r = r_0 e^{i\omega t}$ (for the classic view of the problem see end of the present paragraph). In models corresponding to the quantum mechanical representation, the dipolar moment of transition, i.e., the matrix element of the component of dipolar moment periodically changes with the frequency of conversion, or transition.

Upon observation in the direction of the field, i.e., along the z axis, the π- components will be absent, and only σ- components of two types, polarized in opposite circular direction (longitudinal Zeeman effect) are observed. Observation perpendicular to the field direction (along the x or y axis) reveals both π- and σ- components, both linearly polarized in mutually perpendicular plants (transverse Zeeman effect). The direction of vibrations (electric vector of the emission or absorption of an electromagnetic wave) for π- components coincides with the direction of the z field, and for the σ- components is perpendicular to this direction.

The number of components of each type is easily determined. For the case depicted in Figure 14.3 it is equal to 5. The π- components correspond to the transitions 2-2, 1-1, 0-0, (-1)-(-1) and (-2)-(-2), and two groups of σ- components correspond to the transitions 3-2, 2-1, 1-0, 0-(-1), (-1)-(-2), and 1-2, 0-1, (-1)-0, (-2)-(-1) and (-3)-(-2). The total number of components is 15.

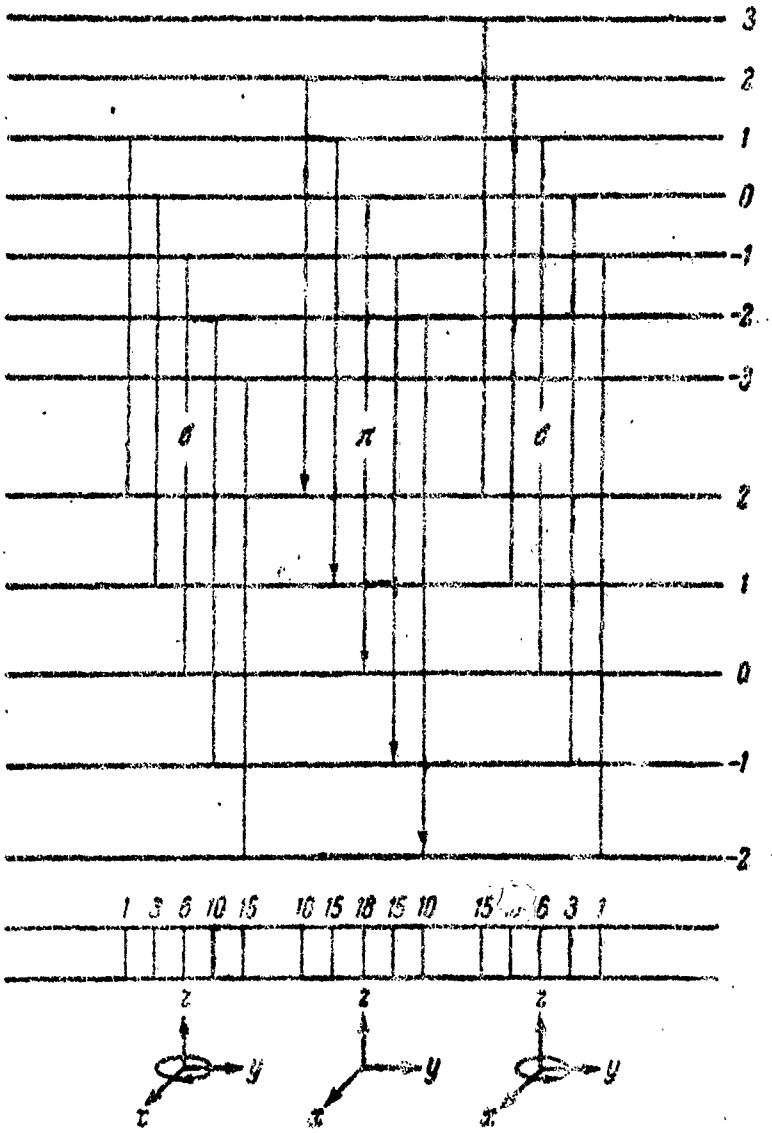

Figure 14.3. Transitions between sublevel levels

J = 3 and J = 2

The disposition of components in the picture of splitting depends upon the relationship between the g-factors of the combining levels. The less the difference between these factors, the closer is the disposition of the components of each group. According to formula (14.8) and the rule of selection, we have the following transitions:

$$\left.\begin{aligned} &m \to m \ (\Delta m = 0) && \Delta E_{m,\,m} = (g_1 - g_2)\mu_B H m, \\ &m+1 \to m \ (\Delta m = +1) && \Delta E_{m+1,\,m} = \\ &\quad = [g_1(m+1) - g_2 m]\mu_B H = [(g_1 - g_2)m + g_1]\mu_B H, \\ &m-1 \to m \ (\Delta m = -1) && \Delta E_{m-1,\,m} = \\ &\quad = [g_1(m-1) - g_2 m]\mu_B H = [(g_1 - g_2)m - g_1]\mu_B H. \end{aligned}\right\} \quad (14.21)$$

The disposition of components is indicated in the lower portion of Figure 14.3 (for the case $g_1 = \frac{6}{7} g_2$). The π-components are disposed symmetrically with respect to the initial position of the non-split line, and the σ-components of each group are disposed symmetrically with respect to the displaced positions $\pm g_1\mu_B H$. The distance between adjacent components within each group is uniform and is equal to $(g_1 - g_2)\mu_B H$, i.e., actually is less with a decrease in the difference $g_1 - g_2$. The entire picture is on the whole symmetrical. The π-components $+m \longrightarrow +m$, $-m \longrightarrow -m$, and the σ-components $m + 1 \longrightarrow m$ and $-m-1 \longrightarrow -m$ are equally distributed with respect to the center; for example, $2 \longrightarrow 2$, $-2 \longrightarrow -2$, and $3 \longrightarrow 2$, $-3 \longrightarrow -2$.

If the g factors of combining levels are equal, all the components of each group coincide, and a particularly simple picture, the simple Zeeman effect, is obtained: the primary spectral line splits into three lines, the Zeeman triplet. This triplet is formed by a non-displaced π-component and two σ-components, symmetrically disposed at a distance $\pm g\mu_B H$ from the former. The picture arising in this case is shown in perpendicular and longitudinal views in Figure 14.4. In the latter case the central non-displaced component, corresponding to vibration of an oscillator along the direction of the field, is absent, and the triplet breaks down into a doublet with $2g\mu_B H$. splitting.

In the case of the simple Zeeman effect formula (14.21) gives the transitions:

$$\left.\begin{aligned} m \to m \quad & \Delta E_{m,m} = 0, \\ m+1 \to m \quad & \Delta E_{m+1,m} = g\mu_B H, \\ m-1 \to m \quad & \Delta E_{m-1,m} = -g\mu_B H. \end{aligned}\right\} \qquad (14.22)$$

With the exclusion of cases of accidental coincidence of the g factor for combining levels, the simple Zeeman effect is obtained in a weak field only in a few completely determined partial cases, namely:

1. In transitions between self-contained levels. In this case S = 0, the complete moment is purely orbital (J = L), and for all self-contained levels g = 1. Zeeman triplets with normal splitting $\mu_B H$ are obtained.

2. In transitions between levels for which the complete orbital moment is equal to zero, L = 0. In this case L = 0, the complete moment is purely spin (J = S), and for all other levels g = 2. Zeeman triplets with $2g\mu_B H$, twice as great as normal, are obtained.

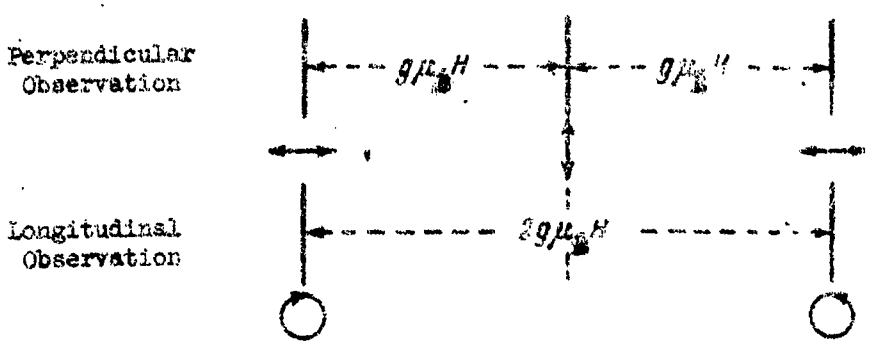

Figure 14.4. Zeeman triplet.

3. In transitions between level J = 1 and J = 0. The second level (m = 0) does not split, but the first splits into three sublevels, with m = 0, $\pm$ 1. The spectral line splits into three components, giving a Zeeman triplet with $g\mu_B H$ splitting, in which the g factor relates to the level J = 1.

In the general case, when $g_1 \neq g_2$, a more complex picture, the complex Zeeman effect, is observed in a weak field.

Extremely varied pictures of splitting are obtained as a function of the value of the difference $g_1 - g_2$ and the values J_1 and J_2, which are discussed in greater detail below, in paragraph 14.4, which is devoted to the types of Zeeman splitting.

Together with the number of components and their distribution, completely determined distribution of the relative intensities of σ- components and π- components with different m values for given values of the quantum numbers J of combining levels is most characteristic of the complex Zeeman effect. This distribution does not depend upon the type of bond.

The general formulas for relative intensities are shown in Table 14.1.

TABLE 14.1

General Formulas for Relative Intensities of Components of the Zeeman Splitting Picture (for transverse observation)

Transitions	$J \to J-1$	$J \to J$
σ- Components $m+1 \to m$	$\frac{1}{4}(J+m+1)(J+m)$	$\frac{1}{4}(J+m+1)(J-m)$
π-Components $m \to m$	$(J+m)(J-m)$	m^2
σ- Components $m-1 \to m$	$\frac{1}{4}(J-m+1)(J-m)$	$\frac{1}{4}(J-m+1)(J+m)$

These formulas first were obtained on the basis of experimental data in combination with the classic representations of Ornstein and Burger in 1924, after which they were derived on the basis of the principle of congruence of Kronig and Goudsmit, independently on Henle, in 1925 (236). They are readily obtained from the basic quantum mechanical formulas for matrix elements of a vector (14), and also may be derived by group theory methods (138).

The intensities are given for transverse observation. In the case of longitudinal observation the intensity of the σ- components is twofold greater than in transverse observation. This is connected with the fact that in longitudinal observation circular polarization is obtained, and transverse vibration along both the x and y axes must be taken into account, but in transverse observation linear polarization is obtained, corresponding to vibration along the axis perpendicular to the direction of observation, and only this vibration need be taken into consideration (for example, vibration along the y axis in observation along the x axis; cf. Figure 14.3). In other words, in the first case two oscillators vibrating along the x and y axes are observed, and in the second case only one of these oscillators is observed.

The intensity of splitting of the components +m and -m symmetrically disposed in the picture is identical, which also derives from the formulas of Table 14.1: upon replacing m with -m the formulas of the row $m \longrightarrow m$ shift by themselves (π- components), and the formulas of row $m + 1 \longrightarrow m$ convert into the formulas of row $m - 1 \longrightarrow m$, and conversely (σ- components). Because of this the splitting picture is symmetrical not only in relation to disposition of components, but also in relation to distribution of intensities. The values of the relative intensities for the case depicted in Figure 14.3 are indicated by the figures above the corresponding components. The problem of distribution of intensities in various cases will be discussed in Paragraph 14.4, in a selective review of types of Zeeman splitting.

It may be noted that the total intensity of all π- components is equal to the total intensity of all σ-components (both groups), which may be proved by summarization of the formulas of Table 14.1 for all values of m from +J to -J. In the particular case of the simple Zeeman effect the intensity of the central π-component is equal to the sum of intensities of both σ- components (having identical intensity).

We investigated the picture of the Zeeman splitting in a weak field and clarified the fact that in the general case a complex Zeeman effect is obtained, leading to a simple Zeeman effect only in individual particular cases, when triplets are observed. Originally it was considered the normal case, in conformance with the classic theory of the Zeeman effect and the data of Lorentz, with the appearance of triplets, and this was referred to as the normal Zeeman effect, with a more complex splitting picture referred to as an anomalous Zeeman effect. This terminology, which occasionally is encountered at present, is outmoded, and it is rational to call the Zeeman effect in the general case of $g_1 \neq g_2$ a complex effect, and to call the particular case in which $g_1 = g_2$ a simple effect, as has been done in the foregoing.

The classic theory does not offer an explanation of the complex Zeeman effect, but it does enable an elementary and very graphic explanation of the simple Zeeman effect, with which the quantum theory is in accord. This explanation is very simple if the concept of Larmor precession of electronic orbits and orbital moments connected with the latter in a magnetic field are utilized, and the explanation is based on investigation of the vibrations of a quasi-elastically bound electron*.

Let us assume an electron under the effect of a quasi-elastic force vibrating at a frequency of ν_0 in a direction comprising a certain angle θ with the direction of the magnetic field (Figure 14.5). This linear vibration may be broken down into vibration along the direction of the field, and vibration in the plan perpendicular to the direction of the field.

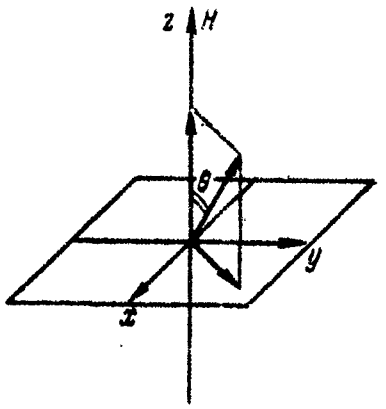

Figure 14.5. Analysis of the vibration of an electron.

---

*) In the classic electronic theory these vibrations are obtained for a point electron in an atom, the positive charge of which uniformly fills a certain sphere (Thompson atomic model); the force acting on the electron in this case is proportionate to its distance from the center of the sphere.

This field does not act upon the vibration along the direction of the magnetic field, and the frequency of vibration ν_0 remains unchanged. We have a linear oscillation oriented in the direction of the field and giving maximal radiation in the plane perpendicular to the field; radiation in the direction of the field is absent. From the quantum point of view, a transition with $\Delta m = 0$, the π- component of the Zeeman triplet with linear polarization along the direction of the field, also corresponds to this oscillator.

Linear vibration perpendicular to the field (cf. Figure 14.5) may be broken down into two circular vibrations of one-half amplitude, with opposed direction of rotation*. With respect to the coordinate system rotating with the Larmor frequency $\nu_L = \frac{eH}{4\pi m_e c}$ (cf. formula (2.70)) they will have the earlier frequency ν_0. Therefore, for circular vibration with direction of rotation coincident with the direction of precession the frequency $\nu_0 + \nu_L$ is obtained, and the frequency $\nu_0 - \nu_L$ is obtained for vibration with opposite direction of rotation. As a result, we obtain two frequencies of vibration, displaced with respect to the original frequency ν_0 by the value

$$\pm \nu_L = \pm \frac{eH}{4\pi m_e c}. \qquad (14.23)$$

---

*) The rotation $x = a \cos 2\pi\nu_0 t$, $y = 0$ may be represented in the form

$$x = \frac{a}{2} \cos 2\pi\nu_0 t + \frac{a}{2} \cos 2\pi\nu_0 t, \qquad y = \frac{a}{2} \sin 2\pi\nu_0 t - \frac{a}{2} \sin 2\pi\nu_0 t,$$

i.e., as the breakdown of circular vibration we have

$$x = \frac{a}{2} \cos 2\pi\nu_0 t, \; y = \frac{a}{2} \sin 2\pi\nu_0 t \quad \text{(rotation from x axis to y axis)},$$

and circular vibration $x = \frac{a}{2} \cos 2\pi\nu_0 t$, $y = -\frac{a}{2} \sin 2\pi\nu_0 t$ (rotation from y axis to x axis).

From the quantum point of view transitions with $\Delta m = \pm 1$: also correspond to a circular oscillator in the xy plane, with frequencies $\nu_0 \pm \nu_L$ which transitions consist of σ- components of Zeeman triplet with circular polarization.

The energy of the emitted or absorbed quants is obtained by multiplication of the corresponding frequencies ν_0 and $\nu_0 \pm \nu_L$ by the constant h. Taking into consideration $\frac{eh}{4\pi m_e c} = \mu_B$ (cf. (2.46)), we obtain for these energies:

$$\left.\begin{array}{ll} \text{Linear Vibration on z Axis} & E_0 = h\nu_0. \\ \text{Circular Vibration in xy Plane} & \left\{\begin{array}{l} E_0 + \Delta E = h\nu_0 + \frac{ehH}{4\pi m_e c} = h\nu_0 + \mu_B H. \\ E_0 - \Delta E = h\nu_0 - \frac{ehH}{4\pi m_e c} = h\nu_0 - \mu_B H. \end{array}\right. \end{array}\right\} \quad (14.24)$$

Exactly the same picture of splitting is obtained as for g = 1 according to (14.22). In this, polarization is determined by the character of vibration of the corresponding oscillators, but the intensity is identical for vibrations along the x, y and z axes, so that transverse observation gives an intensity of π-components equal to the sum of intensities of the σ- components, and in longitudinal observation is twice as great as the intensity of the σ- components.

Thus on the basis of classic representations the simple Zeeman effect with normal splitting $\mu_B H$ is completely explained.

It may be noted that we have coincidence of the frequency of transition between adjacent sublevels at normal splitting $\frac{\Delta E}{h} = \frac{1}{h}\mu_B H$ with frequency $\nu_L = \frac{\mu_B H}{h}$ of precession of orbital magnetic moment $\mu_l = -\mu_B l$ around the direction of the magnetic field. Congruence also is obtained for splitting other than normal. For an arbitrary magnetic moment $\mu = \gamma \hbar J = \frac{\gamma}{\gamma_l}\gamma_l \hbar J = -g\mu_B J$ the frequency of transition between adjacent sublevels in the magnetic

field $\frac{\Delta E}{h} = \frac{g\mu_B H}{h}$, which upon consideration of (2.46) is equal to $\frac{\gamma\mu_B H}{\gamma_l h} = -\frac{\gamma H}{2\pi}$, and coincides with the frequency $\nu = \frac{\omega}{2\pi} = -\frac{\gamma H}{2\pi}$ of precession of this moment, determined by formula (2.59). This congruence is substantial in the visible track of magnetic resonance (cf. Paragraph 14.6 below).

The complex Zeeman effect for spectral lines obtained in transitions between two levels with different values of g, i.e., levels corresponding to different magnetic moments (and consequently, according to visual representation, different angular speeds of precession) cannot be explained by the principle of the classic theory.

All the foregoing of the present paragraph relate to the Zeeman effect for dipolar transitions. For spectral lines obtained in magnetic dipolar transitions the rule of selection is the same as for ordinary dipolar transitions (cf. (4.157)), and the splitting picture is exactly the same. The sole difference consists of the fact that the electric and magnetic vectors of the emitted wave change places; with transverse observation this leads to an exchange of places of the plane of polarization for the π- and σ- components. For spectral lines obtained in quadripolar transitions the rule of selection (4.159) obtains for m, i.e., m may change not only to 0 and $\pm$ 1, but also to $\pm$ 2. The splitting picture becomes complex; the properties of polarization of components also are more complex. This type of Zeeman effect is observed for many prohibited lines, particularly for the 5577 Å line in the spectrum of the aurora polaris corresponding to the quadripolar transition $^1S_0 - {}^1D_2$ for O I.

14.3 The g Factors in the Case of a Weak Field

As we have seen, the magnitude of the Zeeman split depends upon the value of the g factor, and the difference in the g factors for combining levels determines the distance between components in the Zeeman splitting of spectral lines. The value of g for a given level substantially depends upon the type of bond.

In the most important case of normal bond the value of the g factor for a level with a given value of quantum numbers J, S and L is determined by the famous formula of Lande (17)*.

*)Whence the g factor frequently is called the Lande factor.

$$g = 1 + \frac{J(J+1) + S(S+1) - L(L+1)}{2J(J+1)}. \qquad (14.25)$$

In the particular case of purely orbital moment (S = 0, J = L) this formula gives a value of g = 1, and in the particular case of purely spin moment (L = 0, J = S it gives a value of -g = 2 in conformance with the main formulas (14.3) and (14.4), representing a particular case of the general formula (14.8). In the general case, when both L and S are distinct from zero, formula (14.25) leads to different values of g which, however, display completely determined regularity. At given values of L and S, i.e., for a multiple term, the different values of g usually correspond to different values of J.

Table 14.2 contains the values of the g factor for multiples from 2 to 7 (from 1/2 to 3 S) and for values of L from 0 to 4 (i.e., for S-, P-, D-, F- and G-terms). As is customary, the values of g are given for each multiple individually. The values of g are presented in the table in the form of normal and decimal fractions. We see that g is taken both as a value between 1 and 2, at a value less than 1 and a negative value, and also as a value greater than 2. At L > S g increases with an increase in J, at L < S it decreases with an increase in J, and at L = S (which is possible with a whole J) it remains constant and equal to 3/2. At given values of L and S, with the greatest possible J we always have g > 1; for the S term it is equal to 2, after which it decreases with an increase in L, approaching the value g = 1. With the lowest possible J, at L > S we always have g < 1, and it increases with an increase in L, also tending toward a value g = 1, but for L < S it is greater than 2 and increases with an increase in L (attaining its greatest value at L = S - 1 or at L = S = 1/2.

For doublets, and particularly the case of one electron, formula (14.25) assumes a very simple form. In this case S = 1/2, J = L $\pm$ 1/2, and we have

$$\left.\begin{aligned} &\text{at} \quad J = L + \frac{1}{2} \quad g = \frac{L+1}{L+\frac{1}{2}} = \frac{J+\frac{1}{2}}{J}, \\ &\text{at} \quad J = L - \frac{1}{2} \quad g = \frac{L}{L+\frac{1}{2}} = \frac{J+\frac{1}{2}}{J+1}. \end{aligned}\right\} \qquad (14.26)$$

TABLE 14.2

The g Factors with Normal Order of Bond

L	Term	$J=1/2$	$3/2$	$5/2$	$7/2$	$9/2$
0	S	2 2,000				
1	P	$2/3$ 0,667	$4/3$ 1,333			Doublets $S = 1/2$
2	D		$4/5$ 0,800	$6/5$ 1,200		
3	F			$6/7$ 0,857	$8/7$ 1,143	
4	G				$8/9$ 0,889	$10/9$ 1,111

TABLE 14.2 (Cont'd)

The g Factors with Normal Order of Bond

L	Term	$J=1$	2	3	4	5
0	S	2 2,000			Triplets $S=1$	
1	P	$^3/_2$ 1,500	$^3/_2$ 1,500			
2	D	$^1/_2$ 0,500	$^7/_6$ 1,167	$^4/_3$ 1,333		
3	F		$^2/_3$ 0,667	$^{13}/_{12}$ 1,083	$^5/_4$ 1,250	
4	G			$^3/_4$ 0,750	$^{21}/_{20}$ 1,050	$^6/_5$ 1,200

TABLE 14.2 (Cont'd)

The g Factors with Normal Order of Bond

L	Term	$J=1/2$	$3/2$	$5/2$	$7/2$	$9/2$	$11/2$
0	S		2 2,000			Quartets $S=3/2$	
1	P	$8/3$ 2,667	$26/15$ 1,733	$8/5$ 1,600			
2	D	0 0,000	$18/15$ 1,200	$48/35$ 1,371	$10/7$ 1,429		
3	F		$2/5$ 0,400	$36/35$ 1,029	$78/63$ 1,238	$12/9$ 1,333	
4	G			$4/7$ 0,571	$62/63$ 0,984	$118/99$ 1,172	$14/11$ 1,273

TABLE 14.2 (Cont'd)

The g Factors with Normal Order of Bond

L	Term	$J=1$	2	3	4	5	6
0	S		2 2,000			Quintets $S=2$	
1	P	$^{5}/_{2}$ 2,500	$^{11}/_{6}$ 1,833	$^{5}/_{3}$ 1,667			
2	D	$^{3}/_{2}$ 1,500	$^{9}/_{6}$ 1,500	$^{18}/_{12}$ 1,500	$^{6}/_{4}$ 1,500		
3	F	0 0,000	$^{6}/_{6}$ 1,000	$^{15}/_{12}$ 1,250	$^{27}/_{20}$ 1,350	$^{7}/_{5}$ 1,400	
4	G		$^{1}/_{3}$ 0,333	$^{11}/_{12}$ 0,917	$^{23}/_{20}$ 1,150	$^{38}/_{30}$ 1,267	$^{8}/_{6}$ 1,333

TABLE 14.2 (Cont'd)

The g Factors with Normal Order of Bond

L	Term	$J=1/2$	$3/2$	$5/2$	$7/2$	$9/2$	$11/2$	$13/2$
0	S			2 2,000			Sextets $S = 5/2$	
1	P		$12/5$ 2,400	$66/35$ 1,886	$12/7$ 1,714			
2	D	$10/3$ 3,333	$28/15$ 1,867	$68/35$ 1,557	$100/63$ 1,587	$14/9$ 1,556		
3	F	$-2/3$ −0,667	$16/15$ 1,067	$46/35$ 1,314	$88/63$ 1,397	$142/99$ 1,434	$16/11$ 1,455	
4	G		0 0,000	$30/35$ 0,857	$72/63$ 1,143	$126/99$ 1,278	$192/143$ 1,343	$18/13$ 1,385

TABLE 14.2 (Cont'd)

The g Factors with Normal Order of Bond

L	Term	$J=1$	2	3	4	5	6	7
0	S			2 2,000			Septets $S=3$	
1	P		$^{7}/_{3}$ 2,333	$^{23}/_{12}$ 1,917	$^{7}/_{4}$ 1,750			
2	D	$^{6}/_{2}$ 3,000	$^{12}/_{6}$ 2,000	$^{21}/_{12}$ 1,750	$^{33}/_{20}$ 1,650	$^{8}/_{5}$ 1,600		
3	F	$^{3}/_{2}$ 1,500	$^{9}/_{6}$ 1,500	$^{18}/_{12}$ 1,500	$^{30}/_{20}$ 1,500	$^{45}/_{30}$ 1,500	$^{9}/_{6}$ 1,500	
4	G	$-^{1}/_{2}$ −0,500	$^{5}/_{6}$ 0,833	$^{14}/_{12}$ 1,167	$^{26}/_{20}$ 1,300	$^{41}/_{30}$ 1,367	$^{59}/_{42}$ 1,405	$^{10}/_{7}$ 1,429

It may be noted that the sum of these values is 2. For the term ^2P splitting of the $^2P_{3/2}$ level is twice as great as splitting of the $^2P_{1/2}$ level, thus the difference in values of g is equal to $\frac{1}{L + 1/2}$ and decreases with an increase in L, tending toward zero at $L \to \infty$.

Formula (14.25) for the g factor may be derived from graphic considerations of the precession of magnetic moments. The complete magnetic moment μ, obtained as a result of addition of the magnetic moments μ_1 and μ_2 (cf. (2.78)), where $\mu_1 = \gamma_1 \hbar J_1 = -g_1 \mu_B J_1$ and $\mu_2 = \gamma_2 \hbar J_2 = -g_2 \mu_B J_2$ will precess around the direction of the complete mechanical moment $J = J_1 + J_2$, giving the projection (cf. Figure 2.7):

$$\mu_J = \mu_1 \cos(J_1, J) + \mu_2 \cos(J_2, J) = -g_1 \mu_B J_1 \cos(J_1, J) - g_2 \mu_B J_2 \cos(J_2, J). \quad (14.27)$$

According to the relationships $J_2^2 = (J - J_1)^2$ и $J_1^2 = (J - J_2)^2$ we have:

$$\cos(J_1, J) = \frac{J^2 + J_1^2 - J_2^2}{2J_1 J}, \quad \cos(J_2, J) = \frac{J^2 + J_2^2 - J_1^2}{2J_2 J}. \quad (14.28)$$

Substituting (14.28) in (14.27), gives:

$$\mu_J = -\mu_B \left[g_1 \frac{J^2 + J_1^2 - J_2^2}{2J} + g_2 \frac{J^2 + J_2^2 - J_1^2}{2J} \right] =$$

$$= -\mu_B J \left[g_1 \frac{J^2 + J_1^2 - J_2^2}{2J^2} + g_2 \frac{J^2 + J_2^2 - J_1^2}{2J^2} \right] = -\mu_B J g. \quad (14.29)$$

Substituting J^2, J_1^2 и J_2^2 by $J(J+1)$, $J_1(J_1+1)$ and $J_2(J_2+1)$ we have

$$g = g_1 \frac{J(J+1) + J_1(J_1+1) - J_2(J_2+1)}{2J(J+1)} + g_2 \frac{J(J+1) + J_2(J_2+1) - J_1(J_1+1)}{2J(J+1)}. \quad (14.30)$$

The vector

$$\bar{\mu} = \mu_J = -g\mu_B J, \qquad (14.31)$$

representing the average value of magnetic moment of the atom, is oriented within the external magnetic field, giving the projection

$\mu_z = (\mu_J)_z = -g\mu_B J_z = -g\mu_B m$, which, when inserted into (14.1) gives (14.8) with a value of g determined by the general formula (14.31). In the particular case of $J_1 = L$, $J_2 = S$ and also $g_1 = 1$ and $g_2 = 2$, formula (14.31) leads to formula (14.25).

Formula (14.25) (as in the case of the general formula (14.30)) may be obtained by purely quantum mechanical means. For this we must start out from the operator of projection μ_z of complete momentum

$\mu = \mu_L + \mu_S = -\mu_B L - 2\mu_B S$ (cf. (2.48) and (2.55)),

$$\hat{\mu}_z = \hat{\mu}_{Lz} + \hat{\mu}_{Sz} = -\mu_B (\hat{L}_z + 2\hat{S}_z) = -\mu_B (\hat{J}_z + \hat{S}_z) \qquad (14.32)$$

and compute the average value of this operator under the condition with given values of L, S, J and m (cf. (14.13) and (14.14)):

$$\bar{\mu}_z = -\mu_B \int \psi^*_{aJm} (\hat{J}_z + \hat{S}_z) \psi_{aJm}\, dx = -\mu_B m - \mu_B \int \psi^*_{aJm} \hat{S}_z \psi_{aJm}\, dx. \qquad (14.33)$$

The average value of the operator $\hat{S}_z$ is proportionate to m, and as indicated by computation (cf. for example, [131]) is equal to

$$\bar{S}_z = m \frac{1}{2} \frac{J(J+1) + S(S+1) - L(L+1)}{J(J+1)}. \qquad (14.34)$$

Substituting this result in (14.33), and writing $\mu_z = \bar{\hat{\mu}}_z$ according to (14.15) in the form $-g\mu_B m$, we obtain:

$$\mu_z = -\mu_B m - \mu_B \frac{J(J+1) + S(S+1) - L(L+1)}{2J(J+1)} m = -g\mu_B m, \qquad (14.35)$$

whence it follows that we derive (14.25). We have a concrete example of the determination of g (and thus also of the gyromagnetic relationship γ) in formula (14.15).

Other formulas for g factors are obtained for other g factors, expressed through the values of the g factors for accumulated moments and depending upon the order of their addition. In particular, with (j, j), by substituting $J_1 = j_1$ and $J_2 = j_2$ in (14.30), we obtain the formula

$$g = g_1 \frac{J(J+1)+j_1(j_1+1)-j_2(j_2+1)}{2J(J+1)} + g_2 \frac{J(J+1)+j_2(j_2+1)-j_1(j_1+1)}{2J(J+1)}, \quad (14.36)$$

symmetrical with respect to the quantum numbers j_1 and j_2 which determine the moments j_1 and j_2 (the sum of which gives the moment $J = j_1 + j_2$). The factors g_1 and g_2 characterize the original status of electrons and depend upon the quantum numbers l_1, j_1 and l_2, $j_2\left(s_1 = s_2 = \frac{1}{2}\right)$ for these statuses. The values g_1 and g_2 are given by formula (14.26) (in which the following substitutions must be made: $L = l_1$, $J = j_1$ and $L = l_2$, $J = j_2$ and may be taken from Table 14.2 (for doublets). The values of g for the (j, j) bond for two-electron configurations formed by s-, p- and d-electrons are given in Table 14.3. The values of g at various possible values of J (as in Table 14.2, in the form of ordinary and decimal fractions) are given for the given configurations in the rows corresponding to the definite values j_1, j_2 ($j_1 = l_1 \pm 1/2$, $j_2 = l_2 \pm 1/2$).

In the transition from one type of bond to another the g factors of the individual levels gradually change, although the definite rule of sums may be applied. According to this rule the sum of g values for all levels of the configuration considered with the given value J (237, 13) is retained, regardless of the type of bond:

$$\sum_a g_a(J) = \text{const} \qquad (J \text{ given}). \quad (14.37)$$

For example, for the configuration dp (cf. Paragraph 9.1), giving four levels with J = 2, including three levels with J = 3 and J = 1, and one level with J = 4 and J = 0, rule (14.37) is fulfilled for each of these types of levels, for both normal bond and (j, j) bond, as well as for all intermediate cases. In particular, for the

unique level with J = 4, which in the case of normal bond is the $|^3F_4$, level, and in the case of (j, j) bond is the $|(^5/_2, ^3/_2)_4$, level, the value of g remains unchanged and equal to 1.250.

In the case of p^2 configuration the value of g is retained for the unique level with J = 1, and the sum of values of g for two levels with J = 2. In the case of the level with J = 1 $|(^3P_1$ in the case of normal bond, and $|(^3/_2, ^1/_2)_1$ in the case of the (j, j) bond) g = 1.500. For a level with J = 2, we have in the case of normal bond $|g(^3P_2) = 1.500$, $|g(^1P_2) = 1.000$, and in the case of the (j, j) bond $|g[(^3/_2, ^1/_2)_2] = 1.167$, $|g[(^3/_2, ^3/_2)_2] = 1.333$, i.e. in both cases the sum is equal to 2.500.

TABLE 14.3

The g Factors with (j_1, j_2) Bond, for Two-Electron Configurations

Configurations	(j_1, j_2)	$J=1$	2	3	4	5
ss	$(1/2, 1/2)$	$\frac{2}{2,000}$				
ps	$(1/2, 1/2)$	$\frac{4}{3}$ 1,333				
	$(3/2, 1/2)$	$\frac{7}{6}$ 1,167	$\frac{3}{2}$ 1,500			
ds	$(3/2, 1/2)$	$\frac{1}{2}$ 0,500	$\frac{11}{10}$ 1,100			
	$(5/2, 1/2)$		$\frac{16}{15}$ 1,067	$\frac{4}{3}$ 1,333		
pp	$(1/2, 1/2)$	$\frac{2}{3}$ 0,667				
	$(3/2, 1/2)$	$\frac{5}{3}$ 1,500	$\frac{7}{6}$ 1,167			
	$(3/2, 3/2)$	$\frac{4}{3}$ 1,333	$\frac{4}{3}$ 1,333	$\frac{4}{3}$ 1,333		
dp	$(3/2, 1/2)$	$\frac{5}{6}$ 0,833	$\frac{23}{30}$ 0,767			
	$(5/2, 3/2)$	$\frac{16}{15}$ 1,067	$\frac{16}{15}$ 1,067	$\frac{16}{15}$ 1,067		
	$(3/2, 1/2)$		$\frac{58}{45}$ 1,289	$\frac{10}{9}$ 1,111		
	$(5/2, 3/2)$	$\frac{11}{10}$ 1,100	$\frac{109}{90}$ 1,211	$\frac{533}{180}$ 1,239	$\frac{5}{4}$ 1,250	
dd	$(3/2, 3/2)$	$\frac{4}{5}$ 0,800	$\frac{4}{5}$ 0,800	$\frac{4}{5}$ 0,800		
	$(5/2, 3/2)$	$\frac{3}{2}$ 1,500	$\frac{7}{6}$ 1,167	$\frac{13}{12}$ 1,088	$\frac{21}{20}$ 1,050	
	$(5/2, 5/2)$	$\frac{6}{5}$ 1,200	$\frac{6}{5}$ 1,200	$\frac{6}{5}$ 1,200	$\frac{6}{5}$ 1,200	$\frac{6}{5}$ 1,200

In the simplest cases, such as the p^2 configuration, the change in the g factor of individual levels in transition from one type of bond to another may be completely calculated. Observed values of the g factor may serve as a criterion (together with the disposition of levels) of the closeness of bond to the limiting case.

In the interpretation of complex spetra the rule of sums (14.37) may be applied for testing the correctness of this interpretation. If the determined quantum numbers are correctly ascribed to the individual levels, the rule of sums must be fulfilled for levels of the given configuration with the given value J.

14.4. Types of Zeeman Splitting of Spectral Lines

Let us consider the types of Zeeman splitting in greater detail. As mentioned in the foregoing, the type of splitting picture depends strongly upon the difference $g_1 - g_2$, and upon the values J_1 and J_2. In this, the values J_1 and J_2 determine the number of components and the distribution of intensities, and the difference $g_1 - g_2$ determines the distance between components in each group.

The position of individual components in the splitting picture may be found according to formula (14.21); in this, the following outline, which we include for a particular case of combination of $^7F_3$ and $^7G_2$ levels, with normal bond, is adequate for finding the splitting picture. For the first of these levels $g_1 = g(^7F_3) = 1.500$, and for the second $g_2 = g(^7G_2) = 5/6 = 0.833$ (for the value of g cf. Table 14.2).

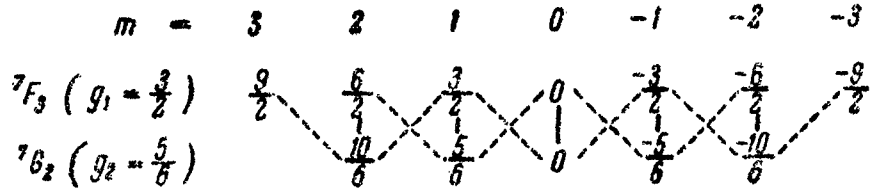

(14.38)

Here the values for both splitting levels, equal to m_1g_1 and m_2g_2 (cf. (14.8)), are given in units of normal splitting $\mu_B H$. The transitions with $\Delta m = 0$, i.e., π-components, are indicated by solid lines, and transitions with $\Delta m = \pm 1$, i.e., σ-components, are indicated by broken lines. The positions of the individual components in relation to the primary line are determined by the difference $m_1g_1 - m_2g_2$. For the π-components ($\Delta m = 0$) we have $\frac{6}{2} - \frac{10}{6} = \frac{8}{6}$, $\frac{3}{2} - \frac{5}{6} = \frac{4}{6}$, $0 - 0 = 0$, etc. As a result we obtain: 8/6, 4/6, 0,

-4/6, -8/6. For the σ- components we similarly obtain: 17/6, 13/6, 9/6, 5/6, 1/6 (at $\Delta m = m_1 - m_2 = +1$) and -1/6, - 5/6, -9/6, -13/6, -17/6 (at $\Delta m = m_1 - m_2 = -1$). The picture obtained, as is emphasized in Paragraph 14.2, is symmetrical with respect to the position of the primary line. The constant distance $g_1 - g_2$ between adjacent components in each group in the given case is equal to

$$\frac{3}{2} - \frac{5}{6} = \frac{4}{6} - \frac{2}{3}.$$

The result obtained is written in the following form, indicating only one-half of the components

$$\frac{(0)\ (4)\ (8)\ 1\ 5\ 9\ 13\ 17}{6}, \qquad (14.39)$$

where the π components are in parentheses, which are lacking in the longitudinal view. The denominator in formulas of this kind (sometimes called the Runge denominator) is the least common multiple of the g_1 and g_2 factors (which in the given case is equal to 6).

The same result may be written in decimal fractions in the form

(0) (0,667) (1,333) 0,167 0,833 1,500 2,167 2,833. (14.40)

The relative intensities of the components may be determined according to the formulas of Table 14.1. Numerical data for the relative intensities of π-components and σ- components (for transverse observation) for the transitions $J \longrightarrow J$ and $J \longrightarrow J - 1$ with whole values of J from 1 to 4 and with half-values of J from 1/2 to 7/2 are shown in Table 14.4. For convenience the intensity values given by the formulas of Table 14.1 are multiplied by 2. For the transitions $J \longrightarrow J$ and $J \longrightarrow J - 1$ a function of intensity different from m is obtained. For the transitions $J \longrightarrow J$ most intense π- components with greatest values, and σ- components with least values $|m|$ are obtained. For the $J \longrightarrow J - 1$ transitions the most intense π-components with the least values of $|m|$, and for σ- components in the group $m + 1 \longrightarrow m$ the intensity increases with an increase in m, and in the group $m - 1 \longrightarrow m$ with a decrease in m.

TABLE 14.4

Relative Intensity of Components of the Zeeman Splitting Picture for Concrete Cases (Transverse Observation)

$J \longrightarrow J$ Transitions (whole values of J and m)

$J \to J$	m $\longrightarrow$ m Transitions (π-components)								
$m =$	4	3	2	1	0	−1	−2	−3	−4
0—0					0				
1—1				2	0	2			
2—2			8	2	0	2	8		
3—3		18	8	2	0	2	8	18	
4—4	32	18	8	2	0	2	8	18	32

$J \to J$	m + 1 $\longrightarrow$ m Transitions (σ-components)							
$m+1 =$	4	3	2	1	0	−1	−2	−3
$m =$	3	2	1	0	−1	−2	−3	−4
1—1				1	1			
2—2			2	3	3	2		
3—3		3	5	6	6	5	6	
4—4	4	7	9	10	10	9	7	4

TABLE 14.4 (Cont'd)

Relative Intensity of Components of the Zeeman Splitting Picture for Concrete Cases (Transverse Observation)

$J \longrightarrow J$ Transitions (half-values of J and m)

$J \to J$	m $\longrightarrow$ m Transitions (π- components)								
	$m =$	$^7/_2$	$^5/_2$	$^3/_2$	$^1/_2$	$-^1/_2$	$-^3/_2$	$-^5/_2$	$-^7/_2$
$^1/_2 — ^1/_2$					0,5	0,5			
$^3/_2 — ^3/_2$				4,5	0,5	0,5	4,5		
$^5/_2 — ^5/_2$			12,5	4,5	0,5	0,5	4,5	12,5	
$^7/_2 — ^7/_2$		24,5	12,5	4,5	0,5	0,5	4,5	12,5	24,5
$J \to J$	m + 1 $\longrightarrow$ m Transitions (σ- components)								
	$m+1 =$ $m =$	$^7/_2$ $^5/_2$	$^5/_2$ $^3/_2$	$^3/_2$ $^1/_2$	$^1/_2$ $-^1/_2$	$-^1/_2$ $-^3/_2$	$-^3/_2$ $-^5/_2$	$-^5/_2$ $-^7/_2$	
$^1/_2 — ^1/_2$					0,5				
$^3/_2 — ^3/_2$				1,5	2	1,5			
$^5/_2 — ^5/_2$			2,5	4	4,5	4	2,5		
$^7/_2 — ^7/_2$		3,5	6	7,5	8	7,5	6	3,5	

TABLE 14.4 (Cont'd)

Relative Intensity of Components of the Zeeman Splitting Picture for Concrete Cases (Transverse Observation)

$J \longrightarrow J - 1$ Transitions (whole values of J and m)

$J \to J-1$	m $\longrightarrow$ m Transitions (π - components)						
$m =$	3	2	1	0	−1	−2	−3
1—0				2			
2—1			6	8	6		
3—2		10	16	18	16	10	
4—3	14	24	30	32	30	24	14

$J \to J-1$	m + 1 $\longrightarrow$ m Transitions (σ - components						
$m+1 =$	4	3	2	1	0	−1	−2
$m =$	3	2	1	0	−1	−2	−3
1—0				1			
2—1			6	3	1		
3—2		15	10	6	3	1	
4—3	28	21	15	10	6	3	1

TABLE 14.4 (Cont'd)

Relative Intensity of Components of the Zeeman Splitting Picture for Concrete Cases (Transverse Observation)

$J \longrightarrow J - 1$ Transitions (half-values of J and m)

$J \to J-1$	m $\longrightarrow$ m Transitions (π-components)						
	$m =$	$^5/_2$	$^3/_2$	$^1/_2$	$-^1/_2$	$-^3/_2$	$-^5/_2$
$^3/_2 — ^1/_2$				4	4		
$^5/_2 — ^3/_2$			8	12	12	8	
$^7/_2 — ^5/_2$		12	20	24	24	20	12
$J \to J-1$	m + 1 $\longrightarrow$ m Transitions (σ-components)						
	$m+1 =$ $m =$	$^7/_2$ $^5/_2$	$^5/_2$ $^3/_2$	$^3/_2$ $^1/_2$	$^1/_2$ $-^1/_2$	$-^1/_2$ $-^3/_2$	$-^3/_2$ $-^5/_2$
$^3/_2 — ^1/_2$				3	1		
$^5/_2 — ^3/_2$			10	6	3	1	
$^7/_2 — ^5/_2$		21	15	10	6	3	1

According to Table 14.4 the relative intensities in the case considered, $^7F_3 - {}^7G_2$, ($J \longrightarrow J - 1$ transition, where J is whole; $J = 3$, $J - 1 = 2$), are 10, 16, 18, 16 and 10 for the π-components, and 1, 3, 6, 10 and 15 for σ- components. The most intense π- component is 0 - 0, for which displacement is equal to 0, and the most intense σ- components are 3 - 2 and (-3)-(-2), for which displacement is equal to $\pm \frac{17}{6} = \pm 2.833$. These components are noted in (14.39) and (14.40), as is customary, by bold face type.

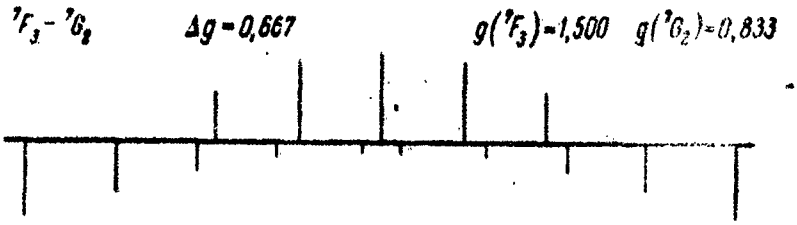

Figure 14.6. Picture of Zeeman Splitting for the Line $^7F_3 - {}^7G_2$.

The picture of splitting for the line $^7F_3 - {}^7G_2$ is shown in Figure 14.6. In the given case $\Delta g = g(^7F_3) - g(^7G_2) = 1.500 - 0.833 = 0.667$. The length of the lines is proportional to the intensities, with the π- components plotted above, and the σ- components below the base line. As may be seen from the figure, the lateral σ- components and the central π- components have the greatest intensity.

The splitting picture may be broken down into three types according to distribution of intensity, which are illustrated in Figure 14.7.

The first type of distribution of intensities is obtained for $J \longrightarrow J - 1$ transitions at $g_J < g_{J-1}$ (Figure 14.7 a). Of the π- components the central values, corresponding to minimal $|m|$ have greatest intensity, and the external values, corresponding to the greatest $|m|$ are the most intense for the σ- components. Thus the

Intensity of π-components drops from the center of the group toward the edges, and the intensity of the σ-components also drops toward the edges of the splitting picture, giving a diminution toward the outside.

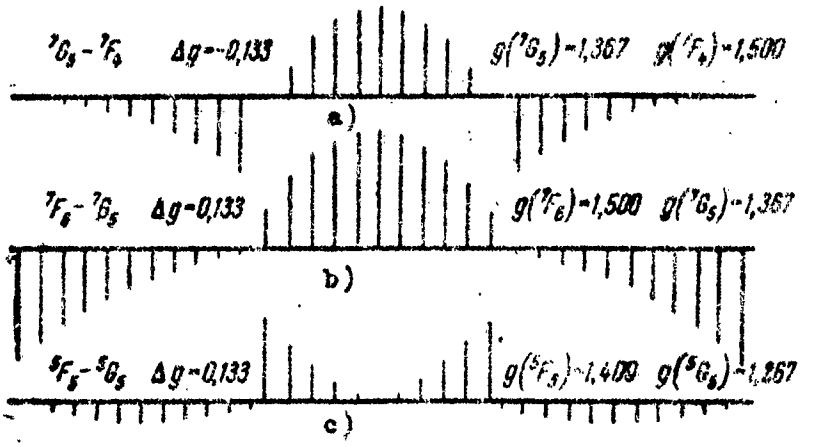

Figure 14.7. Three types of Zeeman splitting:
a) $J \longrightarrow J - 1$, $g_J < g_{J-1}$;
b) $J \longrightarrow J - 1$, $g_J > g_{J-1}$ c) $J \longrightarrow J$.

The second type of distribution of intensities also is obtained for $J \longrightarrow J - 1$ transitions, but at $g_J > g_{J-1}$ (Figure 14.7b, and also Figure 14.6). Of the π-components the central values are the most intense, but of the σ-components the external values are the most intense, because they now correspond to the greatest value of $|m|$. Thus the intensity of π-components drops from the center to the edge of the group, but the intensity of the σ-components drops from the edges of the splitting picture to the center, giving diminution toward the inside.

The third type of distribution of intensities is obtained for the $J \longrightarrow J$ transitions (Figure 14.7 c). Of the π-components the most intense values are at the edges, and of the σ-components those located in the center of each group and corresponding to the least value of $|m|$ are the most intense. Thus the intensity of the π-components increases from the center toward the edges, and the intensity of the σ-components drops from the center toward both sides of each group.

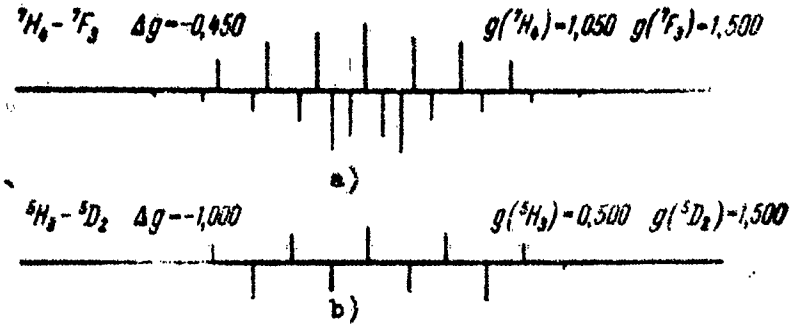

Figure 14.8. Picture of Zeeman splitting at large $|g_1 - g_2|$ differences:

a) Overlapping of σ- components of both groups;
b) Exact coincidence of σ- components of both groups.

Figure 14.7 contains characteristic examples of three types of splitting corresponding to $^7G_5 - {}^7F_4$, $^7F_6 - {}^7G_5$ and $^5F_5 - {}^5G_5$ transitions, for which $|\Delta g| = 0.133$. With an increase in the difference $|\Delta g| = |g_1 - g_2|$ the intervals between components in each group increase, and the internal components of the two groups of σ- components gradually approach each other. The internal σ- components and the external π- components begin to overlap; an example is the $^7F_3 - {}^7G_2$ transition considered above (cf. Figure 14.6), relating to the second type of distribution of intensities. At large $|g_1 - g_2|$ differences the σ-components of the two groups also overlap (Figure 14.8 a); in this case exact coincidence of the σ-components of both groups is possible (Figure 14.8 b).

The presence of the three types of distribution of intensities described usually is placed at the basis of classification of the types of splitting. According to Back, these types of splitting are indicated as types I, II and III.

Type I	Type II	Type III
$J \rightarrow J - 1,\ g_J < g_{J-1}$	$J \rightarrow J - 1,\ g_J > g_{J-1}$	$J \rightarrow J$

Back includes the limiting cases of Zeeman triplets under type IV.

A somewhat more detailed classification is applied by Harrison (240); he indicates Types I, II, III as types 1, 2, and 3 for the case of even multiples (half-value of J) and types 4, 5 and 6 for the case of odd multiples (whole value of J). The limiting cases of the Zeeman triplet are indicated as type 7 a at $J - 1 = 0$ ($1 \rightarrow 0$ transition), and as type 7 b at $g_1 = g_2$.

Conclusions may be drawn with respect to the values J and g for combining levels according to experimentally observed splitting pictures. Two types of cases must be distinguished: the case of a completely resolved splitting picture, in which adjacent components are separated from each other, and the case of incompletely resolved pictures, in which adjacent components run together, frequently observed at small values of the difference $|\Delta g| = |g_1 - g_2|$.

In both cases the general character of distribution of intensities usually enables determination of whether there are combining levels with identical J values or different J values, and in the case of different J values the level with the greatest g may be determined. With complete resolution of the splitting picture the J and g values may be easily found.

The possibility of finding the values of J and g for individual energy levels on the basis of analysis of the splitting picture is of great importance in studying the Zeeman effect for interpretation of complex atomic spectra. If the levels of the configurations which may be expected for the spectrum of the investigated atom or ion are known from theoretical considerations or from comparison with analogous spectra, selection of the values of J and g may resolve the problem of the type of bond which exists, and it may be determined whether the bond is close to the normal quantum numbers L and S.

It must be noted that in finding the values of L and S not tables of the type of Table 14.2, but tables in which the values of the g factor are listed in mounting order, and the level giving this value of g is given are used. Tables of this type are drawn up individually for levels of even and odd multiple terms, up to the multiplicity values $x = 10$ and 11.

The values of J and g with complete resolution of the splitting picture are determined as follows.

The number of components also gives the value J. For $J \longrightarrow J$ transitions the number of σ-components in each group is equal to 2J, and the number of π-components is equal to 2J - 1 for half-values of J, and 2J for whole values of J (taking into account prohibition of the transition $m = 0 \longrightarrow m = 0$; cf. Tables 14.2 and 14.4). For $J \longrightarrow J - 1$ transitions both the number of σ-components in each group and the number of π-components is equal to 2J - 1 (cf. diagram (14.38 corresponding to J = 3, 2J - 1 = 5).

The values of the g_1 and g_2 factors are determined on the basis of measurement of the distance between adjacent components $e = |g_1 - g_2|$ and the distance of 2f between the most intense σ-components of both groups. For these values we have the following relationships for the various types of transitions:

$$\left.\begin{array}{llll} J \to J-1 & g_1 < g_2 & g_1 = f + (J-1)e, & g_2 = f + Je, \\ J \to J-1 & g_1 > g_2 & g_1 = f - (J-1)e, & g_2 = f - Je, \\ J \to J & & g_1 = f + \frac{e}{2} & g_2 = f - \frac{e}{2}. \end{array}\right\} \qquad (14.41)$$

Actually, for $J \longrightarrow J - 1$ transitions the most intense σ-components correspond to $|m|$, equal to $j - 1$. Their positions, according to (14.21) will be (in $|\mu_B H$ units):

$$\left.\begin{array}{ll} \text{at } m = J-1 & \text{transition } m+1 = J \to m = J-1) \\ & (g_1 - g_2)(J-1) + g_1, \\ \text{at } m = -J+1 & \text{transition } m-1 = -J \to m = -J+1) \\ & -(g_1 - g_2)(J-1) - g_1, \end{array}\right. \qquad (14.42)$$

and the difference between these positions is equal to

$$2[g_1 + (g_1 - g_2)(J-1)] = 2f. \qquad (14.43)$$

Hence $f = g_1 - e(J - 1)$ at $g_1 < g_2$, $g_2 - g_1 = e$ and $f = g_1 + e(J - 1)$ at $g_1 > g_1$, and $g_1 - g_2 = e$, giving us the final result (14.41) for $J \longrightarrow J - 1$ transitions.

For $J \longrightarrow J$ transitions the most intense σ-components correspond to transitions with minimal $|m|$; namely (cf. Table 14.4):

transition $1/2 \longrightarrow -1/2$ and $-1/2 \longrightarrow 1/2$ at half-value J
transition $1 \longrightarrow 0$, $0 \longrightarrow -1$ and $-1 \longrightarrow 0$, $0 \longrightarrow 1$ at whole J.

In the first case we find the positions of the components according to (14.21):

$$\left.\begin{array}{lll} \text{at } m = -\frac{1}{2} & \left(\text{transition } m+1 = \frac{1}{2} \rightarrow m = -\frac{1}{2}\right) & \frac{1}{2}(g_1 + g_2), \\ \text{at } m = \frac{1}{2} & \left(\text{transition } m-1 = -\frac{1}{2} \rightarrow m = \frac{1}{2}\right) & -\frac{1}{2}(g_1 + g_2). \end{array}\right\} \quad (14.44)$$

The difference between these positions is equal to:

$$g_1 + g_2 = 2f. \quad (14.45)$$

Then, taking $g_1 > g_2$, we find:

$$g_1 + g_2 = (g_1 - g_2) + 2g_2 = e + 2g_2 = 2f, \quad g_1 + g_2 =$$

$$= 2g_1 - (g_1 - g_2) = 2g_1 - e = 2f \quad (14.46)$$

and obtain the result (14.41) for $J \longrightarrow J$ transitions. The same result also is obtained in the second case, if the distance between components is taken at $1 \longrightarrow 0$ (position of g_1) and $0 \longrightarrow 1$ (position of g_2), or the distance between the components $0 \longrightarrow -1$ (position of g_2) and $-1 \longrightarrow 0$ (position of g_1) or finally, the distance between centers of the pairs $1 \longrightarrow 0$, $0 \longrightarrow -1$ and $0 \longrightarrow 1$, $-1 \longrightarrow 0$ (cf. Figure 14.9).

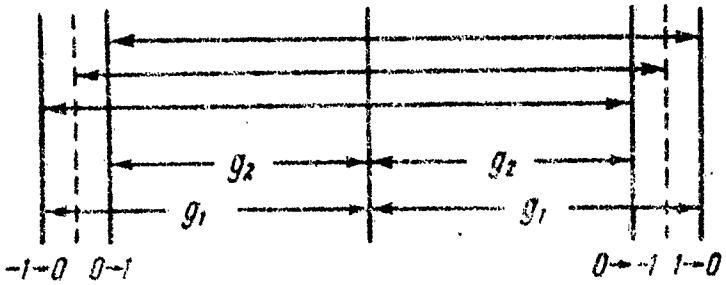

Figure 14.9. Distance between components of the splitting picture for $J \longrightarrow J$ transitions at whole-value J.

The picture of splitting depicted in Figure 14.6 may serve as an example. Let us assume that the values J and g are unknown. We have the distributions of intensities at which the central π-component and the extreme σ-components of both groups are most intense, i.e, the case $J \longrightarrow J - 1$, $g_1 > g_2$. The number of components in each group is equal to $5 - 2J - 1$, whence $J_1 = 3$, $J_2 = J - 1 = 2$. The distance between adjacent components is $e = 0.667$, and the distance between the most intense σ-components is $2f = 5.666$. Thence according to (14.41) (second row), we have:

$$g_1 = 2{,}833 - 2 \cdot 0{,}667 = 1{,}500; \quad g_2 = 2{,}833 - 3 \cdot 0{,}667 = 0{,}833.$$

In the case of incomplete resolution of the splitting picture identical determination of all the values J_1, J_2, g_1 and g_2 is impossible. However, in this case many conclusions may be made relative to the properties of the combining levels. In addition to relating transition to one of three main types according to the character of distribution of intensity, it is possible to measure the distance $2f'_\sigma$ between the centers of gravity of two nonresolved maximums, which form two groups of σ-components. For transition of the type $J \longrightarrow J$ the group of π-components also gives two nonresolved maximums due to the fact that at minimal values of $|m|$ the intensity is minimal and a barrier is formed; the distance $2f_\pi$ between centers of gravity of these maximums gives the second parameter characterizing the given transition, which at a given J enables determination of the values g_1 and g_2 (238).

14.5. The Zeeman Effect in Strong and Intermediate Fields

In the foregoing paragraphs we discussed the Zeeman effect in weak fields in detail, in which the magnitude of the Zeeman effect is much less than the distance between adjacent levels of energy (cf. (14.9)). Let us consider now the case of a strong field, when conversely, the magnitude of the Zeeman splitting is much greater than this distance (cf. (14.10)).

For electronic magnetic moments of the atom with which we are concerned in the present chapter, having an order of magnitude of μ_B and for which the conditions (14.9) and (14.10) have been described, the case in which the distance between adjacent levels is determined by multiple line structure is of greatest importance. In other words, the most important case is the normal bond, when there are close levels forming multiple terms with multiple line splitting

of the order $\zeta(L, S)$, in which $\zeta(L, S)$ is the multiple line split factor (cf. Paragraph 9.5). At a distance between adjacent levels on the order of $\zeta(L, S)$ the conditions (14.9) and (14.10) assume the form:

$$\text{weak field} \qquad \mu_B H \ll \zeta(L, S), \tag{14.47}$$

$$\text{strong field} \qquad \mu_B H \gg \zeta(L, S). \tag{14.48}$$

In the latter case it is impossible to speak of independent splitting of each level of a given multiple line term: a splitting picture general for all levels is obtained. As a result, in a very strong field a Zeeman triplet for the entire multiple as a whole, with normal splitting $\mu_B H$ is observed instead of a complex Zeeman effect for each line of the multiple. This effect, first discovered by Paschen and Back in 1912 (174, 16) received the name of the Paschen-Back effect. It occurs in sufficiently strong magnetic fields for light atoms in which the factor of multiple splitting ζ is small and may fulfill the conditions of (14.48).

The Paschen-Back effect is readily explained on the basis of graphic representations of the precession of magnetic moments; the results obtained coincide with the results of the quantum mechanical theory in the strict sense.

The physical conditions (14.48) mean that the supplementary energy $-(\mu_L H)$ and $(\mu_S H)$ of orbital and spin magnetic moments in the magnetic field on the order of $\mu_B H$ is much greater than the energy of spin orbital interaction

$$A(LS) = \zeta(L, S)(LS) \quad [\text{cf. (9.35)}].$$

According to graphic representation the angular velocities of precession.

$$\omega_L = -\gamma_L H = -\frac{\mu_L}{\mu_B^{(\text{orb})}} H, \quad \omega_S = -\gamma_S H = -\frac{\mu_S}{\mu_B^{(\text{spin})}} H \tag{14.49}$$

(cf. (2.59), (2.45) and (2.54)) of orbital and spin moments $\boldsymbol{L}$ and $\boldsymbol{S}$ in the direction of the field become much greater than their angular velocity of simultaneous precession in the direction of the complete moment $\boldsymbol{J}$ (cf. Figure 2.8, c, $J_1 = L$, $J_2 = S$). As a result, the magnetic field breaks the bond (L, S) and each of the vectors $\boldsymbol{L}$ and $\boldsymbol{S}$ precess around the direction of the magnetic field independently, giving the quantum projections m_L and m_S for this direction. Thus at the same time, as in the case of a weak field, the complete moment $\boldsymbol{J}$ precesses around its direction (Figure 14.10, a; angular velocity of precession

$$\omega_J = -\gamma H = -\frac{\mu_J}{M_p^{(\text{comp})}} H$$

much less than the angular velocity of precession $\boldsymbol{L}$ and $\boldsymbol{S}$ around $\boldsymbol{J}$) the moments $\boldsymbol{L}$ and $\boldsymbol{S}$ precess around this direction separately in a strong field (Figure 14.10, b). In the latter case the quantum number J completely loses meaning: the complete moment of the atom $\boldsymbol{J}$ is not retained, and the condition of the system is characterized by the quantum numbers L, m_L and S, m_S.

The formulas (14.3) and (14.4) hold for the supplementary energy in a magnetic field for L and for S separately, and may be written in the form:

for L $$\Delta E_{m_L} = \mu_B H m_L. \qquad (14.50)$$

for S $$\Delta E_{m_S} = 2\mu_B H m_S. \qquad (14.51)$$

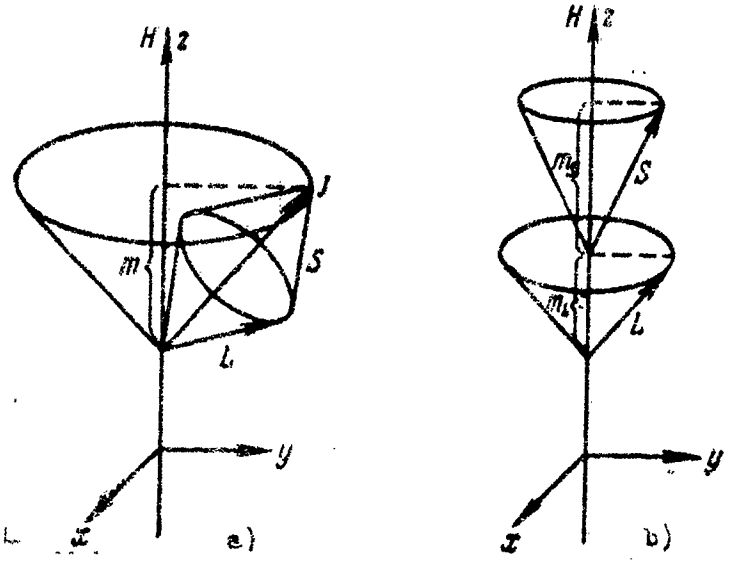

a) In a weak field;

b) In a strong field;

Figure 14.10. Precession of moments.

The complete supplementary energy in a magnetic field is equal to

$$\Delta E_{m_L, m_S} = \Delta E_{m_L} + \Delta E_{m_S} =$$
$$= \mu_B H (m_L + 2m_S). \qquad (14.52)$$

Because m_L is always whole and $2m_S$ also is whole (even at half-value m_S) sublevels are obtained, the distances between which are whole multiples of the normal split $\mu_B H$.

Formula (14.52) may be obtained directly by quantum mechanical procedures by starting out with the type of operator of supplementary energy in the magnetic field (cf. (14.11) and (14.32)). When the spin-orbital interaction $A(\hat{L}\hat{S})$ may be considered small in comparison to the operator $\hat{V} = \mu_B H(\hat{L}_z + 2\hat{S}_z)$, the projections of L and S in the direction of the field must be quantized separately, the proper value of the operator $\hat{L}_z$ is equal to m_L, the proper value of the operator $\hat{S}_z$ is equal to m_S, and the average value of the operator $\hat{V}$ in the condition of the given values of L, m_L and S, m_S coincide with its proper value and are equal to (cf. (14.12) through (14.15)):

$$\bar{\hat{V}} = \int \psi^*_{\alpha L m_L S m_S} \mu_B H (\hat{L}_z + 2\hat{S}_z) \psi_{\alpha L m_L S m_S} dx =$$
$$= \mu_B H \int \psi^*_{\alpha L m_L S m_S} (m_L + 2m_S) \psi_{\alpha L m_L S m_S} dx = \mu_B H (m_L + 2m_S). \qquad (14.53)$$

The rule of selection

$$\Delta m_L = 0, \pm 1 \qquad (14.54)$$

and

$$\Delta m_S = 0. \qquad (14.55)$$

hold for the quantum numbers m_L and m_S for ordinary dipolar radiation.

These rules of selection are partial cases of the general rules of selection (4.157), with prohibition of $\Delta m_S = \pm 1$, transitions for the spin magnetic quantum number m_S, which are possible in the general case.

This is connected with the fact that the electric dipolar moment of the atom P depends solely upon the spatial coordinates (cf. (4.33)). Stating the wave function ψ_{m_L, m_S} in the form

$$\psi_{m_L, m_S}(y, \sigma) = \psi_{m_L}(y)\,\psi_{m_S}(\sigma), \qquad (14.56)$$

where $\psi_{m_L}(y)$ is a function of the spatial coordinates y, and $\psi_{m_S}(\sigma)$ is a function of the spin coordinates σ, we obtain for the matrix element of the dipolar moment the expression

$$P_{m_L m_S, m'_L m'_S} = \sum_{\sigma} \int \psi^*_{m_L m_S}(y, \sigma)\, P(y)\, \psi_{m'_L m'_S}(y, \sigma)\, dy =$$

$$= \int \psi^*_{m_L}(y)\, P(y)\, \psi_{m'_L}(y)\, dy \sum_{\sigma} \psi^*_{m_S}(\sigma)\, \psi_{m'_S}(\sigma), \qquad (14.57)$$

which reverts to zero due to the orthogonality of the functions $\psi_{m_S}(\sigma)$ and $\psi_{m'_S}(\sigma)$, if $m_S \neq m'_S$, which also gives the rule of selection (14.55). It is noted that the given conclusion is correct in the case of a sufficiently strong field when it is possible, ignoring spin-orbital interaction, to represent the wave function in the form of (14.56).

As a result of the rules of selection (14.54) and (14.55), in a strong field, with transition between sets of levels of two multiple terms a nondisplaced π-component (at $\Delta m_L - \Delta m_S = 0$) and two symmetrically disposed displaced σ-components (at $\Delta m_L = \pm 1$, $\Delta m_S = 0$) are obtained, i.e., a Zeeman triplet with normal splitting $\mu_B H$. is obtained. Thus in a strong field the simple Zeeman effect with normal splitting must be observed.

The outline of transitions and the picture of splitting obtained are depicted at the right in Figure 14.11 for the particular case of transition between sublvels of the term ^2P(L = 1, S = 1/2) and sublevels of the term ^2S (L = 0, S = 1/2). The values m_L, m_S are indicated for each sublevel, also the values of their sums $m = m_L + m_S$.

At the given values of m_L and m_S the supplementary energy in a magnetic field is determined by formula (14.52). It is noted that for the term ^2P we have $\Delta E_{m_L m_S} = 0$ as well as at $m_L = 1$, $m_S = -1/2$ and at $m_L = -1$, $m_S = 1/2$.

The splitting picture discussed is obtained when spin-orbital interaction may be completely ignored. If this interaction must be taken into consideration as a correction under the conditions of (14.48), its magnitude may be determined readily, being equal to

$$\Delta E'_{m_L m_S} = \zeta(L, S)\, m_L m_S. \qquad (14.58)$$

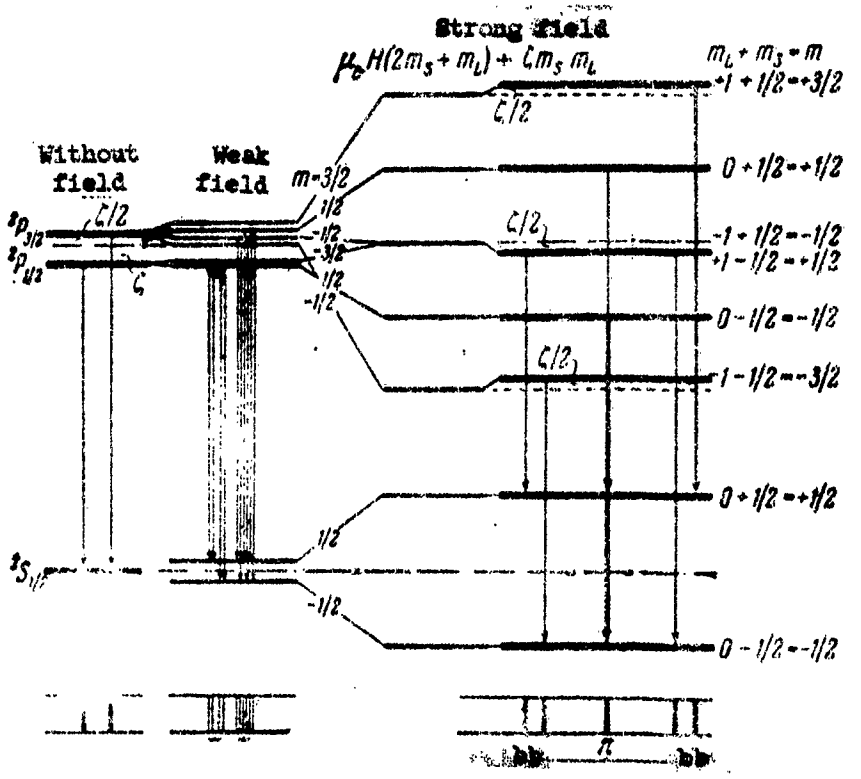

Figure 14.11. Comparison of splitting in a weak field and in a strong field, for $^2P - {}^2S$ transition.

Adding (14.58) and (14.52) we obtain the complete supplementary energy in a strong magnetic field

$$\Delta E_{m_L m_S} = \mu_B H (m_L + 2m_S) + \zeta (L, S)\, m_L m_S. \quad (14.59)$$

Formula (14.58) may be obtained easily by starting out from the expression for the energy of spin-orbital interaction

$$A (LS) = \zeta (L, S) (LS) = \zeta (L, S)\, LS \cos (L, S). \quad (14.60)$$

At the same time, as in a weak field, (LS) has the completely determined value $1/2 [J(J + 1) - S(S + 1) - L(L + 1)]$ (cf. (2.86) and 9.35) in a strong field, when L and S precess in independent manner and the average value $\overline{(LS)} = LS \cos (L, S)$ must be used. The cosine of the angle between the vectors L and S may be represented in the form (cf. Figure 14.10 b).

$$\cos (L, S) = \cos (x, L) \cos (x, S) +$$

$$\cos (y, L) \cos (y, S) + \cos (z, L) \cos (z, S).$$

In averaging this expression the average value of the first two members in the right-hand portion is equal to zero (angles L and S with axis x and axis y change independently), and in the third member

$$\cos(z, L) = \frac{m_L}{L}, \cos (z, S) = \frac{m_S}{S} \quad \text{and thus}$$

$$\zeta (L, S) \overline{(LS)} = \zeta (L, S)\, LS \overline{\cos (L, S)} =$$

$$\zeta (L, S)\, LS \frac{m_L}{L} \frac{m_S}{S} = \zeta (L, S)\, m_L m_S,$$

i.e., we obtain expression (14.58).

Taking into account the second member in (14.59), conditioned by spin-orbital interaction, leads to the fact that sublevels with different values of m_L, m_S will not be equi-distant and the splitting picture in transition between the sublevels of the two terms will only approximate the Zeeman triplet, differing from it by the presence of the structure of individual components of the triplet.

For example, in the discussed case of $^2P - {}^2S$ (Figure 14.11) transition, for the term ^2P the member $\zeta (^2P)\, m_L m_S$ gives the

correction $^1/_2\zeta(^3P)$ for the sublevels $m_L = -1$, $m_S = 1/2$ and $m_L = 1$, $m_S = -1/2$, and the correction $^1/_2\zeta(^3P)$ for the coinciding sublevels $m_L = -1$, $m_S = 1/2$ and $m_L = 1$, $m_S = -1/2$; the sublevels $m_L = 0$, $m_S = -1/2$ and $m_L = 0$, $m_S = 1/2$ retain their position. The π-component in the splitting picture retains its position, but the σ-components will be doubled, with splitting equal to $\zeta(^3P)$. Displacement of sublevels and splitting of σ-components are indicated in the right-hand portion of Figure 14.11. A similar picture is observed for the first member of the main Id series, represented by the doublet $2s\,^2S_{1/2} - 2p\,^2P_{1/2,\,3/2}$ with 0.34 cm^{-1} splitting (cf. Table 8.7), which according to (8.29) is equal to $^3/_2\zeta_{2p} = {}^3/_2\zeta(^3P)$, whence $\zeta(^3P) = 0{,}23\ cm^{-1}$. . In a magnetic field of 20,000 gauss, according to (14.6) the distance $2\mu_B H$ between σ-components is $2 \cdot 0.934\ cm^{-1} = 1.87\ cm^{-1}$; the splitting of these components is equal to $\zeta(^3P) = 0{,}23\ cm^{-1}$.

To the present time we have discussed the Zeeman effect in weak and strong fields, independently. With a gradual increase in the magnetic field, a gradual change in the splitting picture of the levels and of the spectrual lines also occurs, consisting of a transition from the Zeeman effect in weak fields to the Zeeman effect in strong fields. The magnitude of Zeeman splitting in intermediate, or medium fields, in transition from weak to strong, is on the same order as multiple-line splitting

$$\mu_B H \sim \zeta(L, S), \qquad (14.61)$$

and this greatly complicates the splitting picture. The distance between components does not change in proportion to the magnetic field, and the different components behave differently. Complete computation of the splitting of terms is complicated and leads to unwieldy formulas, although a qualitative picture may be obtained for intermediate fields without calculation through comparison of Zeeman sublevels and limiting cases of weak and strong fields.

As we have seen, the complete mechanical moment $\boldsymbol{J}$ is not retained in the transition from a weak to a strong field (cf. page 42); however, the complete projection of mechanical moments of the atom in the direction of the field remains constant, and retains its value m. In a weak field this projection is $m = m_J$, where m_J acquires $2J + 1$ values ($m_J = J, J - 1, \ldots . -J$) for the levels with given J. In a strong field the complete projection is equal to the sum of the projections m_L and m_S of the moments $\boldsymbol{L}$ and $\boldsymbol{S}$:

$$m = m_L + m_S, \tag{14.62}$$

where $m_L = L, L - 1, \ldots, -L$ and $m_S = S, S - 1, \ldots, -S$. For the given term the number of sublevels in a weak field and in a strong field is equal to the number $(2L + 1)(2S + 1)$ and is identical for the two cases, regardless of the conditions. In this, the value of m is retained for each sublevel.

Retention of the value of the complete projection is connected with the axial symmetry of homogeneous magnetic field. In the case of axial symmetry this projection is quantized independently of the intensity of the magnetic field. In this, the operator $J_z = L_z + S_z$ of the complete projection of mechanical moments coincides with the operator of infinitely small revolution around the direction of the field.

Knowledge of the value of m is insufficient for comparison of sublevels in a weak and strong field. Unequi-vocal comparison is obtained if in addition to retention of m the rule that different levels with the same value of m must not intersect in the transition from a weak field to a strong field is taken into consideration. The given rule is a particular case of the general rule of nonintersection of levels. According to this rule, established by Wigner and Neumann, (203) if several quantum numbers are retained in the transition from one limiting case to another, levels with identical sets of these quantum numbers may not intersect.

Bearing in mind the retention of m and the rule of intersection, comparison of sublevels in a weak field with sublevels in a strong field may be easily accomplished.

This type of comparison is indicated in Figure 14.11 for the case of the ^2P term. In a weak field the level $^2P_{1/2}$ splits into two

sublevels with $m = m_J = 1/2, -1/2$, and the $^2P_{3/2}$ splits into four sublevels with $m = m_J = 3/2, 1/2, -1/2, -3/2$; a total of $(2L + 1)(2S + 1) = 3 \cdot 2 = 6$ sublevels is obtained. In a strong field 6 sublevels are obtained also, which we have discussed in the foregoing, of which two ($m_L = 1$, $m_S = -1/2$ and $m_L = -1$, $m_S = 1/2$) coincide. The lower sublevel, with $m_J = -1/2$, converts into a sublevel with $m_L = 0$, $m_S = -1/2$, and the upper sublevel, with $m_J = -1/2$ converts into a sublevel with $m_L = -1$, $m_S = +1/2$, because there may not be an intersection of these sublevels in intermediate fields. Similarly, the lower sublevel, with $m_J = 1/2$, converts into a sublevel with $m_L = 1$, $m_S = -1/2$, and the upper sublevel, with $m_J = 1/2$, converts into a sublevel with $m_L = 0$, $m_S = 1/2$. Finally, the sublevel with $m_J = -3/2$ and $m_J = 3/2$ convert into sublevels with $m_L = -1$, $m_S = -1/2$ and $m_L = 1$, $m_S = 1/2$, respectively. The disposition of sublevels is indicated in Figure 14.11, taking into consideration the factor of multiple-line splitting ζ, in accordance with (14.59).

In other cases comparison is made in a similar manner. Change in the splitting picture of spectral lines in transition from a weak field to a strong field also may be traced, but will not be discussed at the present time.

Our discussion has related to the case of a normal bond. Breaking of the (j, j) bond in a strong magnetic field also may be discussed in exactly the same manner as well as the bond of any given two vectors $\boldsymbol{J}_1$ and $\boldsymbol{J}_2$, forming the resultant vector $\boldsymbol{J} = \boldsymbol{J}_1 + \boldsymbol{J}_2$. Supplementary energy in a strong magnetic field breaking the (J_1, J_2) bond may occur similarly to (14.52) (cf. (14.8)):

$$\Delta E_{m_1 m_2} = \mu_B H (g_1 m_1 + g_2 m_2). \qquad (14.63)$$

In distinction from (14.52), however, the distance between the sublevels obtained will not, generally speaking, be whole multiples of the normal split $\mu_B H$, and Zeeman triplets with normal splitting will not be obtained.

Breaking of the bond of various moments may occur in several stages. For example, for triplet terms of two-electron configurations the bond between L and S will break first, as has been described in the foregoing, after which, in sufficiently strong fields, the bond between l_1 and l_2 and between s_1 and s_2 break (complete effect of Paschen-Back).

The practical Zeeman effect in strong and intermediate fields is observed for light atoms and also for high terms of heavy atoms, i.e., in cases in which splitting conditioned by spin-orbital interaction is not very great and does not exceed several cm^{-1}.

In closing the present paragraph it may be noted that in comparison of splitting of energy levels in magnetic fields of various intensities very useful rules of sums may be established for groups of sublevels with given values of quantum number m, retaining application in a magnetic field, namely the rule of sums for the g factor and the rule of sums for the magnitude of splitting (cf. (13)).

14.6. General Characteristics of Magnetic Resonance

Let us consider at this point magnetic resonance, i.e., forced transitions between sublevels of Zeeman splitting. On page 1 the general characteristics of magnetic resonance, correct for both electronic magnetic resonance conditioned by electronic magnetic moments, and also nuclear magnetic resonance conditioned by nuclear moments, plus rotation magnetic resonance conditioned by rotational magnetic moments were given*.

Transition between two Zeeman sublevels of a level of given value J and having identical even number is possible, according to the rule of selection (4.154), only in a magnetic dipole and in quadripolar radiation. However, in the radio frequency range of the spectrum the probability of quadripolar transitions in comparison with magnetic dipolar transitions is very small (the probability of quadripolar transitions much faster than the factor ν^2 decreases with frequency), and only the magnetic dipolar transitions, the probability of which is determined by the magnetic moments of these transitions (cf. (4.73)) need be taken into consideration. Actually, according to (4.85) the ratio of the probability of quadripolar transitions to the

---

*) Magnetic resonance, conditioned by nuclear moments, will be discussed under Chapter 16, and that due to rotational moments are discussed in Chapter 19.

probability of magnetic dipolar transitions has the following order of magnitude

$$\varepsilon = \frac{A^{(\text{quad})}}{A^{(\text{mag})}} = \frac{B^{(\text{quad})}}{B^{(\text{mag})}} = 3\left(\frac{\nu}{c}\right)^2 \frac{|Q|^2}{|\mu|^2}. \qquad (14.64)$$

For the wave length $\lambda = 1\ cm\left(\frac{\nu}{c} = 1\ cm^{-1}\right)$ we find, assuming

$Q \approx ea^2 \approx 5 \cdot 10^{-10} \cdot 10^{-16} = 5 \cdot 10^{-26}$, $\mu \approx \mu_B \approx 10^{-20}$,

that the ratio ε is on the order of 10^{-10}, i.e., it is very small.

Thus the transitions between sublevels of Zeeman splitting are conditioned by magnetic dipolar radiation.

It is very important that the probability of spontaneous transitions between Zeeman sublevels is insignificantly small, and that spontaneous emanation is lacking. This is generally characteristic of transitions with radiation in the radio frequency range of the spectrum; spontaneous emanation is lacking under ordinary conditions, and may be observed only in exclusive cases*. As a rule, forced transitions -- absorption and forced emanation are observed in the radio frequency range; magnetic resonance constitutes a partial case of forced transitions in the radio frequency range of the spectrum.

The probability of spontaneous transitions between sublevels of Zeeman splitting may be evaluated easily, starting out with the formula for magnetic dipolar radiation (cf. (4.85)), $A^{(\text{mag})} = 3 \cdot 10^{29}\left(\frac{\nu}{c}\right)^3 |\mu|^2$. For splitting caused by electronic magnetic moments having the Bohr magneton order of $\mu_B \approx 10^{-20}$ erg/gauss (cf. (2.47)) we obtain, assuming $\lambda = 4\ cm$, $\frac{\nu}{c} = 0.25\ cm^{-1}$ (which corresponds to the magnetic field $H \approx 5{,}000$ gauss),

$A^{(\text{mag})} \approx 3 \cdot 10^{29} \cdot 0.25^3 \cdot 10^{-40}\ \text{sec}^{-1} \approx 5 \cdot 10^{-13}\ \text{sec}^{-1}$

i.e., the value of $A^{(\text{mag})}$ is very small. The value of $A^{(\text{mag})}$ is still smaller for transitions due to nuclear and rotational moments on the order of the nuclear magneton.

---

*) These conditions are realized for cosmic radiation; cf. Chapter 16.)

According to the rule of selection (4.157), as for ordinary electronic dipolar radiation transitions with change of the magnetic quantum number m not greater than unity, i.e., $|\Delta m| \leqslant 1$ are possible for magnetic dipolar radiation.

By virtue of this rule of selection only transitions between adjacent sublevels of Zeeman splitting are resolved, as indicated for values of J from 1/2 to 2 in Figure 14.12. Transitions upward are absorption, and transitions downward are forced emanation. Transitions with unit change of m, $\Delta m = \pm 1$, correspond to circular vibration in the xy plane, perpendicular to the direction of the permanent magnetic field, caused by Zeeman splitting. These transitions may be evoked by an alternating magnetic field with resonant frequency

$$\nu = \frac{1}{h} |E_m - E_{m\pm1}|,$$ perpendicular to the permanent magnetic

field. Thus magnetic resonance occurs under the action of an alternating magnetic field of frequency

$$\nu = \frac{1}{h} |E_m - E_{m\pm1}|, \qquad (14.65)$$

perpendicular to the permanent magnetic field.

According to the general formula (4.172), in the case of

$\Delta m = m_1 - m_2 = \pm 1$ only the matrix elements $A_x \pm iA_y$ of the vector

components are different from zero. The following matrix elements (cf. (4.175) and others) are different from zero

$$(m_1 | \mu_x \pm i\mu_y | m_2) = \int \psi^*_{m_1}(\varphi)(\mu_x \pm i\mu_y)\psi_{m_2}(\varphi)\, d\varphi \qquad (14.66)$$

at $m_1 = m_2 \pm 1$, which means that from the point of view of graphic

representations this transition corresponds to magnetic circular oscillators in the plane xy, having the frequency (14.65). The vibration of these oscillators may be excited by a magnetic field of the same frequency, located in the plane xy.

Special notice must be made of the fact that the transitions considered are magnetic dipolar transitions and occur under the effect of an alternating magnetic field, while ordinary electrical dipolar transitions occur under the effect of an alternating electrical field.

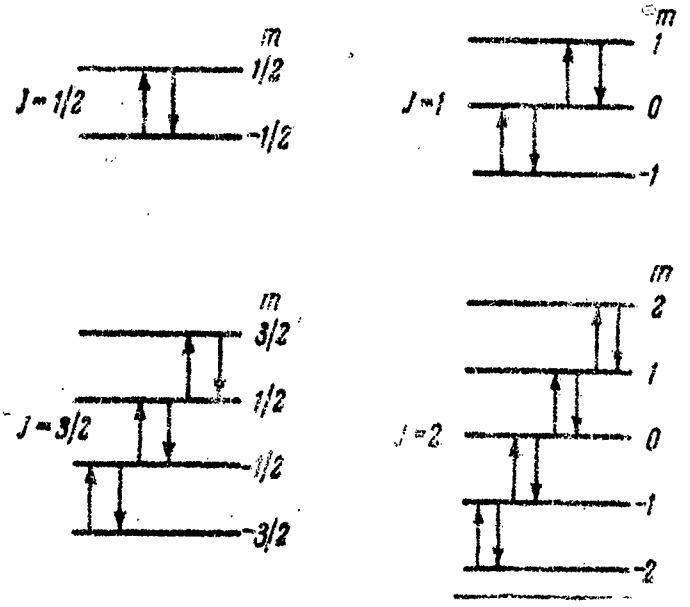

Figure 14.12. Transitions between adjacent sublevels of Zeeman splits.

Whereas the frequency of transition between adjacent sublevels of Zeeman splitting coincides with the frequency of precession of the magnetic moment around the direction of the permanent magnetic field H, as mentioned in the foregoing, the condition of magnetic resonance is coincidence of the frequency of the alternating magnetic field perpendicular to the permanent magnetic field with the frequency of precession.

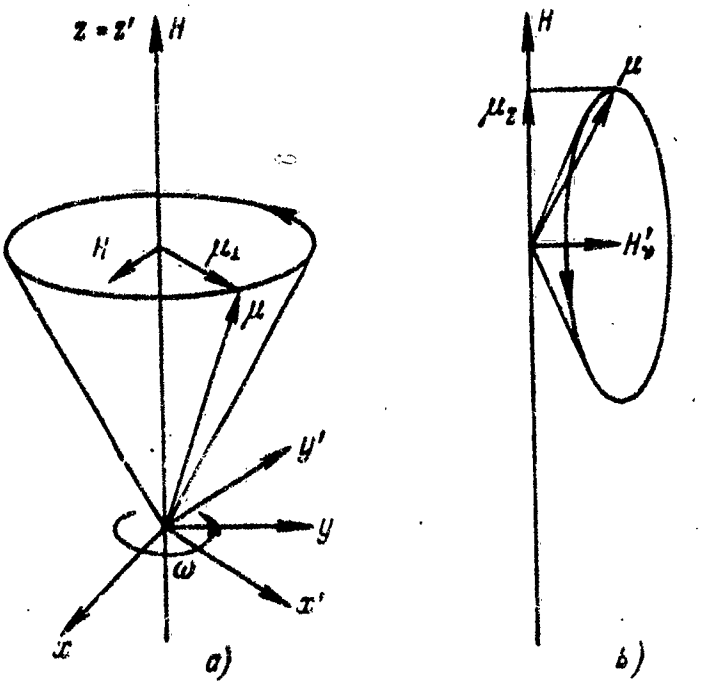

Figure 14.13. Effect of a perpendicular magnetic field on a precessing magnetic moment:
a) precession around the field H; ;
b) supplementary precession around the field H'_y..

From the purely classic viewpoint radiation of frequency equal to the frequency of precession is connected with the rotation of the components of magnetic moment $\mu_\perp$, perpendicular to the axis of precession, i.e., the direction of H . Changes in the magnitude of projection of the magnetic moment in the direction of H. in the case of forced transition may be understood according to the graphic representation, utilizing the principle of congruence. For this we consider the effect of the perpendicular magnetic field H_y upon the magnetic moment in the moving coordinate system precessing around the direction of H with angular velocity $\omega = -\gamma H$ (Figure 14.13 a). As we have seen in Chapter 2, the change $\left(\frac{dM_p}{dt}\right)_{\text{rot}}$ of mechanical moment in this system, in the absence of effects other than the H field, is equal to zero. In the presence of a perpendicular field H_y , creating the supplementary moment of force $[\mu, H_y] = [\gamma M_p, H_y]$ we obtain

$$\left(\frac{dM_p}{dt}\right)_{\text{rot.}} = [\gamma M_p, H_v]. \tag{14.67}$$

The alternating field H_v with frequency $\nu = \frac{\omega}{2\pi}$ may be analyzed into two magnetic fields H_v' and H_v'' of the same frequency, rotating in opposite directions with angular velocity ω and $-\omega$*. The field H_v', rotating with angular velocity ω, may be constant with respect to the moving system, but the magnetic moment must precess around the direction H_v' (cf. Figure 14.13 b), and consequently it will change its orientation with respect to the H field, i.e., μ_z will change. The gradual change in orientation of magnetic moment in the classic theory would correspond to an intermittant change of this orientation and the projection μ_z in the quantum theory. Specifically, with the original orientation parallel to H the magnetic moment gradually changes to antiparallel orientation. For the spin moment of the electron ($s = 1/2$) this corresponds to quantum transition from the sublevel $m_s = 1/2$ to the sublevel $m_s = -1/2$.

There are two different means of observation of magnetic resonance: measurement of the effect of radiation upon molecular beams, and measurement of the absorption of radiation by a substance.

---

*) For example, vibration along the x axis, $H_x = H_0 \cos \omega t$, may, upon addition of a field along axis y equal to zero, be analyzed in the following form:

$$H_x + iH_y = H_x + i \cdot 0 = \left(\frac{H_0}{2}\cos \omega t + \frac{H_0}{2}\cos \omega t\right) + i\left(\frac{H_0}{2}\sin \omega t - \frac{H_0}{2}\sin \omega t\right) =$$

$$= \frac{H_0}{2}(\cos \omega t + i \sin \omega t) + \frac{H_0}{2}(\cos \omega t - i \sin \omega t) = \frac{H_0}{2} e^{i\omega t} + \frac{H_0}{2} e^{-i\omega t}.$$

The first member represents the magnetic field rotating from the x axis to the y axis, with angular velocity ω, and the second member the magnetic field rotating from the y to the x axis, with angular velocity $-\omega$.

The first method consists of a beam of the investigated particles (having magnetic moment), deflected in a definite manner in permanent magnetic fields (which for this purpose are made nonhomogeneous) and impinging upon the instrument registering the particles, and is subjected to the effect of radio frequency radiation. If under the effect of the magnetic field of radiation, transitions occur between sublevels of Zeeman splitting, which does occur in the presence of resonance, i.e., at coincidence of the frequency of the field of radiation with the frequency of transition, then the particles with projection of magnetic moment modified as a result of the transition are deflected differently and no longer impinge upon the instrument. Thus the weakening of the beam of investigated particles observed at resonant frequencies is measured.

Figure 14.14 shows a typical diagram of apparatus for investigation of magnetic resonance in molecular beams (42). The beam of particles from source S passes through the nonhomogeneous permanent magnetic fields A and B, deflecting the particles in opposite directions and focusing the beam, which impinges on the registering instrument I. A homogeneous permanent field is created by magnet C between magnets A and B, and an alternating radio frequency magnetic field (radiation field) evoking transitions is established perpendicularly to the last named. When the frequency of the alternating field does not coincide with the frequency of transitions, a completely determined stream of particles falls upon the receiving instrument, and in the case of coincidence of frequencies all the particles for which projection of the magnetic moment changed as a result of transitions between sublevels of Zeeman splitting are deflected differently by the second nonhomogeneous field B and do not enter the receiver.

It is important that the change in intensity of the beam is proportionate to the total number of transition processes from the original sublevels equal to the sum of the number of all the absorption processes and all processes of forced emanation. For example, in the case of splitting of a level with $J = 1$ in a magnetic field (cf. Figure 14.12) the change in intensity of the beam occurs as a result of both $-1 \longrightarrow 0$ and $0 \longrightarrow 1$ (absorption) transitions, and $0 \longrightarrow -1$ and $1 \longrightarrow 0$ (emanation) transitions. In the given case the probability of all these transitions is equal.

The relative probability of the transitions is given by the formulas of Table 14.1 for the case $J \longrightarrow J$ and $m \pm 1 \longrightarrow m$, which also hold for transitions between sublevels of the same level. Because of this, Table 14.4 may be utilized in concrete instances.

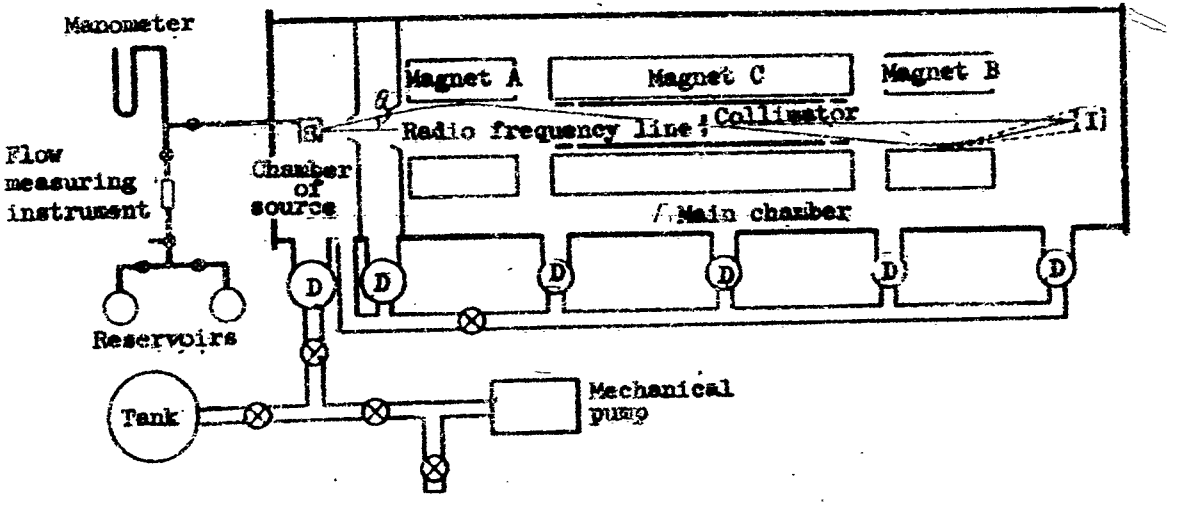

Figure 14.14. Diagram of apparatus for investigating magnetic resonance in molecular beams:
S - source; I - registering instrument; D - diffusion pumps.

The magnetic resonance method with molecular beams is extremely sensitive, and enables a very high degree of precision to be attained. Its most important aspect is that the effect of a radio frequency field on free particles is studied. However, from the experimental point of view it is very difficult because working with molecular beams, especially in magnetic fields, is complicated, particularly in respect to the requirement of special vacuum technology.

The second method of observation of magnetic resonance consists of measurement of the absorption of radio frequency radiation by a substance placed in a permanent, homogeneous magnetic field. The radio frequency magnetic field evokes transitions between sublevels of Zeeman splitting, with both $m \longrightarrow m+1$ and $m+1 \longrightarrow m$ transitions, i.e., both absorption and forced emanation occur. For example, in the simplest case of Zeeman splitting of a level with $J = 1/2$ (cf. Figure 14.12) this corresponds to the transitions $-1/2 \longrightarrow 1/2$ and $1/2 \longrightarrow -1/2$. The observed absorption is the difference between absorption and forced emanation. The coefficient of absorption, measured by experiment, is determined by formula (5.98) and contains the

$\alpha = \frac{h\nu}{kT}$, factor, and in the given case $h\nu = E_{m_1} - E_{m_2}$ is the

difference in energy of the Zeeman split sublevels. Magnetic resonance may be observed as a result of high sensitivity of contemporary radio technological methods, even in the case of very close Zeeman split sublevels. Despite the presence of experimental methods, study of absorption in the radio frequency range does not differ in principle from study of absorption in the optical range, while the magnetic resonance method with molecular beams has the substantial advantage that not radiation, but change in the status of particles subjected to the effect of radiation is studied.

Study of magnetic resonance by the absorption method is considerably simpler than the molecular beam method, and also enables attainment of high resolving power and very high precision of measurement. This method usually is used in the study of substances in solid and liquid state, which on one hand enables different conclusions to be made relative to the condensed state of the substance, but on the other hand requires introduction of many corrections in the determination of the properties of individual particles. The values of magnetic moments determined for particles interacting with the surrounding particles may be distinguished from the values of these moments for free particles.

It is noted that usually in the observation of magnetic resonance not the frequency of radiation causing the transitions, but the intensity of the permanent magnetic field in which these transitions

are observed is varied (by the molecular beam, or absorption method). Thus to satisfy the relationship $h\nu = \Delta E_m - \Delta E_{m-1} = g\mu_B H$ the value ν is kept constant and H is varied. Therefore the spectra are obtained not on a frequency scale (or wave length scale), but on a scale of intensity of the magnetic field.

14.7. Investigation of Electronic Magnetic Resonance by the Atomic Beam Method

Measurement of magnetic resonance in atomic beams, being a particular case of molecular beams*, enables the electronic maguetic moments of atoms in basic condition to be measured with very high precision, on the order of one hundred-thousandth. A particularly simple case is that of atoms with one external s-electron, for which the main level is the $ns\,^2S_{1/2}$ level (atoms of hydrogen, alkali metals, plus Cu, Ag and Au; cf. Table 7.2). The transitions $-1/2 \longrightarrow 1/2$ and $1/2 \longrightarrow -1/2$ are observed (cf. Figure 14.12), which are connected with a change in the orientation of the spin moment of the electron in the magnetic field. The main result of experiments with these atoms (and also with atoms in other basic conditions, particularly in the condition $np\,^2P_{1/2}$) is that the factor g for electron spin magnetic moment is different from the value 2, to which the theory of Dirac leads, i.e., the magnitude of magnetic moment is not equal to the Bohr magneton μ_B(cf (2.56)). This anomaly of the magnetic moment of the electron, as indicated in Chapter 6, is caused by radiation corrections which may be found through utilization of the quantum electrodynamics methods. The theoretical value of the magnetic moment $\mu_{el} = \frac{1}{2} g\mu_B$ of the electron when using corrections on the order of α and α^2, where α is the constant of fine structure (6.48) is

$$\mu_{el} = \frac{g}{2}\mu_B = \left(1 + \frac{\alpha}{2\pi} - 0{,}328\,\frac{\alpha^2}{\pi^2}\right)\mu_B = 1{,}0011596\,\mu_B \quad (14.68)$$

Fine measurements of Zeeman splitting for the basic condition $1s\,^2S_{1/2}$ of the hydrogen atom by the magnetic resonance method with an atomic beam leads to the value

---

* For terminology see page 1.

$$\frac{g}{2} = \frac{\mu_{el}}{\mu_B} = 1{,}001146 \pm 0{,}000012, \qquad (14.69)$$

which approximates the theoretical value (14.68). It conforms even more closely to the value g/2 of (14.68), measured directly for free electrons (cf. (14.81). This conformity, together with coincidence of the theoretical and experimental values of the shift is S-level for the n = 2 status of the hydrogen atom is a basic proof of the correctness of deductions of quantum electrodynamics obtained on the basis of consideration of radiation corrections.

The experimental value of the g/2 factor for H^1 is equal to 1.001128 ± 0.000012, for D^2 is 1.001128 ± 0.000030, for He^4 is 1.001117 ± 0.000020 and for Li^6 and Li^7 is 1.00114 ± 0.00012, i.e., in all cases the correction obtained is equal approximately to $\frac{\alpha}{2\pi} = 0.00116$. The relative change in electron mass connected with the hydrogen atom must be taken into account in making comparison with a free electron. This change in mass is $1.8 \cdot 10^{-5}$, and gives a correction of +0.000018, which leads to the value (14.69) for a free electron.

Theoretical computation of the value g/2 for He^4 in the basic condition $^3S_1$ leads to the value 1.0011044, which also agrees very well with the experimental value introduced in the above, 1.001117 ± 0.000020.

The method of magnetic resonance in atomic beams may be used in investigation of the picture of Zeeman splitting of energy levels not only in weak fields, but also in intermediate, and strong fields. Along with study of Zeeman splitting of main levels of atoms the picture of splitting of excited levels also may be investigated in principle if a sufficient concentration of these atoms is created in the beam. Investigation of this type was carried out by Lamb and his associates in studying the shift of S-levels (248, cf. Paragraph 6.8); namely, study of Zeeman splitting of levels with n = 2 enabled the value of this shift to be determined with high precision.

The peculiarity of Zeeman splitting of excited levels of the hydrogen atom consist of the fact that there are closely adjacent levels with different values of l. For n = 2 we have the levels $2s\,^2S_{1/2}$, $2\,^2P^o_{1/2}$ and $2\,^2P^o_{3/2}$ (cf. Figure 6.14). In this, the magnitude

of splitting in magnetic fields is on the order of several thousand gauss of the distance between the $^2P^o_{1/2}$ and $^2P^o_{3/2}$ levels. The picture of the splitting of levels with n = 2 is shown in Figure 14.15. In this, the even level $^2S_{1/2}$ splits independently of uneven levels $^2P^o_{1/2}$ and $^2P^o_{3/2}$, for which we have the case of splitting in intermediate fields, corresponding to the middle portion of Figure 14.11. In the given case this splitting may be computed easily, taking into account the interaction between two levels with m = 1/2 and two levels with m = -1/2. In all, we have two even levels with m = 1/2 and m = -1/2, indicated by α and β, and six uneven levels with m = 3/2, 1/2, -1/2, -3/2 (from $^2P^o_{3/2}$) and m = 1/2, -1/2 (from $^2P^o_{1/2}$), indicated, by a, b, c, d, e and f. In distinction from the case of transitions between sublevels of the same level, possible only with magnetic dipolar radiation, ordinary electric dipolar transitions with the rule of selection $\Delta m = 0, \pm 1$, are possible only with magnetic dipolar radiation between sublevels of the levels ^2S and $^2P^o$, the same as in the case of splitting of spectral lines in the optical range of the spectrum. In this, forced transitions with $\Delta m = 0$ are evoked by radio frequency electric fields parallel to the permanent magnetic field, and transitions with $\Delta m = \pm 1$ by a field perpendicular to the permanent magnetic field. According to the rule of selection the following transitions are possible:

$$\left.\begin{array}{ll} \Delta m = 0 & \alpha - e,\ \alpha - b; \qquad \beta - f,\ \beta - c, \\ \Delta m = \pm 1 & \alpha - f,\ \alpha - c,\ \alpha - a;\ \beta - e,\ \beta - d,\ \beta - b \end{array}\right\} \quad (14.70)$$

In the experiments of Lamb hydrogen atoms in a beam were excited, as described in Paragraph 6.8, by means of electronic impulse. Atoms in excited state $2^2P^o_{1/2}$ and $2^2P^o_{3/2}$ incandesce (vysvechivayutsya) immediately due to optical transition at the basic level $1^2S_{1/2}$, and atoms in the $2^2S_{1/2}$ excited state are metastable and remain in the beam, falling into the magnetic field in sufficiently large numbers. In this, atoms located at the sublevel β (m = -1/2) are less stable than

at the $|\alpha\rangle$ $(m = 1/2)$ sublevel due to the possibility of transitions without irradiation under the effect of a perpendicular electric field* at the sublevel e, with which the sublevel $|\beta\rangle$ intersects approximately at H = 540 gauss. As a result the atomic beam is polarized; it contains almost exclusively atoms in the condition $|\alpha(2\,^2S_{1/2}, m = 1/2)\rangle$ condition. Careful measurement of the frequency of $|\alpha\rangle$ - e and $|\alpha\rangle$ - f (forced emanation) in a field H = 1,160 gauss for hydrogen (frequency of transition 2395 Mc) enabled the precise value (6.87) of the shift of the S-level to be found. Through measurement of the frequency of transition $|\alpha\rangle$ - a (absorption) in a 630-gauss field (frequency of transition 10,795 Mc) the value of the energy difference $2^2P^0_{3/2} - 2^2S_{1/2}$ for deuterium (6.88) was found. It may be noted that in addition to electric dipolar transitions magnetic dipolar transition $|\alpha\rangle - |\beta\rangle$ in the form of a very abrupt resonance maximum was observed, which was utilized for calibration of the magnetic field; the frequency of this transition, according to formulas (14.4) and (14.68) is equal, with a very good degree of approximation, to

$$\left| \Delta E_{1/2} - \Delta E_{-1/2} = g\mu_B H = 2\left(1 + \frac{\alpha}{\pi}\right)\mu_B H. \right. \qquad (14.71)$$

Transitions between the $|\alpha\rangle$ sublevel of the level $^2S_{1/2}$ and the sublevels e, f, and a of the levels $^2P_{1/2}$ and $^2P_{3/2}$ are much less abrupt due to the great natural width of the P level, connected with the resolved optic transitions

$$|2\,^2P^0_{3/2} - 1\,^2S_{1/2}| \text{ and } 2\,^2P^0_{1/2} - 1\,^2S_{1/2},$$

which occur with considerable probability. According to Table 6.6, this probability is equal to $6.25 \cdot 10^8$ sec^{-1} which, according to formula (4.128), gives a level width equal to

$$\left| \Delta\nu = \frac{A}{2\pi} = \frac{6{,}25 \cdot 10^8}{6{,}28} \right| \text{sec}^{-1} \approx 100 \text{ mc} \qquad (14.72)$$

---

*) Due to the law of induction, this field acts on rapidly moving particles flying through a magnetic field. For transitions with irradiation, under the effect of an electric field, cf. Chapter 15.

The width is increased further due to the superfine structure. However, due to symmetry of line contour the value of maximum intensity (with the introduction of small corrections for the existing low asymmetry) may be found with very high precision, which also creates the possibility the precise values of the frequency of transitions.

14.8. Investigation of Electronic Magnetic Resonance by the Absorption Method

The method of electronic paramagnetic resonance (EPR), often called simply paramagnetic resonance, is a very important and absorption method. Electronic paramagnetic resonance, discovered by Zavoyskiy (cf. page 2), is observed in the microwave range of the radio frequency spectrum, in that the distance between adjacent levels of Zeeman splitting on the order of $\mu_B H$ and in fields on the order of 1,000 gauss is on the order of cm^{-1} (cf. (14.6)). The cause of simultaneous absorption and paramagnetism of a substance is the orientation of electronic magnetic moments by the external magnetic field. At heat equilibrium the colonization of sublevels of the Zeeman splitting is determined by the formula of Bolzmann (5.10)*

$$n_m = n_0 A e^{-\frac{\Delta E_m}{kT}} = n_0 A e^{\frac{\mu_z H}{kT}} = n_0 A e^{-\frac{g\mu_B H m}{kT}}, \quad (14.73)$$

where ΔE_m is the supplementary energy in the magnetic field (cf. (14.1) and (14.8)), n_0 is the number of particles, and A is a constant (determined by the condition that the total number of particles at all levels is equal to n_0). As a result of a somewhat larger population of levels with lower values m the substance in the magnetic field has, at $\mu \neq 0$, a resultant magnetic moment, i.e., it is magnetized. For the same reason the number of transitions $m \longrightarrow m+1$, i.e., the number of absorption processes, is greater than the number of transitions $m+1 \longrightarrow m$, i.e., the number of processes of forced emanation; this also leads to a value of the adduced coefficient of absorption (cf. formula (5.68)) different from zero and deriving from formulas (5.84, (5.91) and (5.98), which also determine the absorption observed in the experiment and representing the difference between absorption and forced emanation. The coefficient of absorption for the transition

---

*) In this it is taken into account that the statistical weight to all sublevels is identical and equal to 1 (degeneration in the magnetic field is deducted. The energy reading in (14.73) is taken relative to the non-split level $\Delta E_m = 0$.

$\overline{m} \longrightarrow m + 1$, according to (5.98), is equal to

$$\varkappa_\nu = \frac{1}{c} h\nu n_m \frac{h\nu}{kT} B_{m,\, m+1}(\nu), \qquad (14.74)$$

where $B_{m,\, m+1}(\nu)$ is the probability of absorption for magnetic dipolar irradiation. In the microwave range the coefficients of absorption are sufficiently large to be measured even at relatively low concentrations of paramagnetic particles.

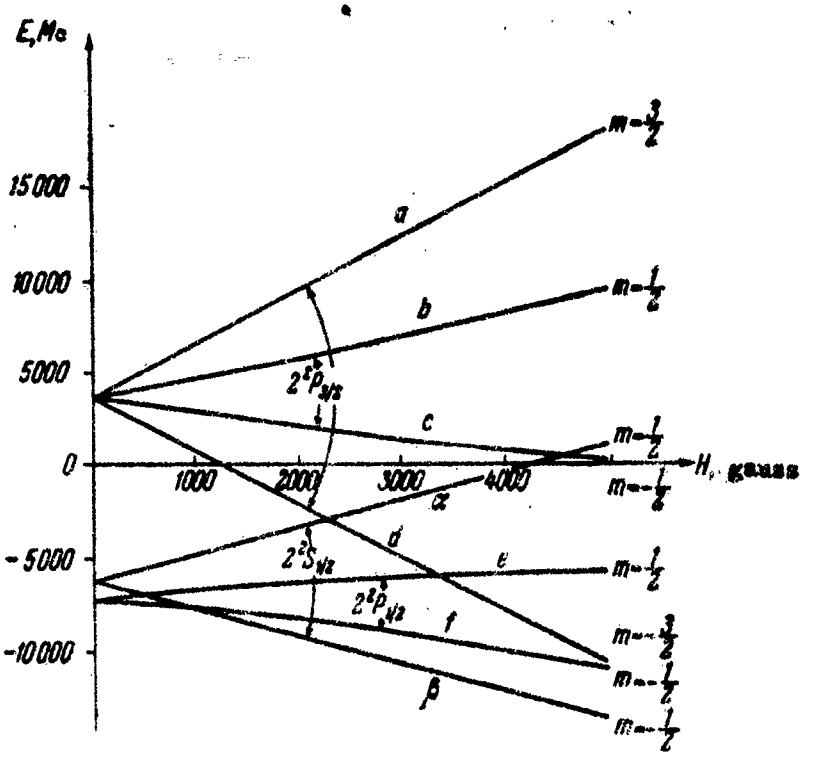

Figure 14.15. Splitting of the n = 2 level of the hydrogen atom in a magnetic field.

The order of magnitude of the probability $B_{m,\, m+1}(\nu)$ of the transition from sublevel m to sublevel m + 1 may be easily evaluated, and starting out from this evaluation the order of magnitude of the coefficient of absorption may be found.

The spectral probability of absorption relating to the unit of interval of frequency enters into formula (14.74) and according to (5.126) is equal to

$$B_{m,\,m+1}(\nu) = \frac{B_{m,\,m+1}}{\Delta\nu}, \qquad (14.75)$$

where $B_{m,\,m+1}$ is the integral probability of absorption, and $\Delta\nu$ is the width of the spectral line for the transition $m \longrightarrow m+1$. Expressing $B_{m,\,m+1}$ through the magnetic moment of transition, according to formulas (4.8) and 4.73) we obtain ($g_m = g_{m+1} = 1$)

$$B_{m,\,m+1}(\nu) = \frac{1}{\Delta\nu}\frac{c^3}{8\pi h\nu^3}A_{m+1,\,m} = \qquad (14.76)$$

$$= \frac{1}{\Delta\nu}\frac{c^3}{8\pi h\nu^3}\frac{64\pi^4}{3hc^3}\nu^3\left|\mu_{m,\,m+1}\right|^2 = \frac{1}{\Delta\nu}\frac{8\pi^3}{3h^2}\left|\mu_{m,\,m+1}\right|^2.$$

The magnetic moment of transition is on the order of magnitude of the magneton of Bohr μ_B, i.e., $|\mu_{m,\,m+1}|^2 \approx 10^{-40}$ erg/gauss (cf. (2.47)). At a line width on the order of 10^8 gauss (i.e. $\frac{\Delta\nu}{\nu} = 1/100$ at $\nu = 10^{10}$ gauss)

$$B_{m,\,m+1}(\nu) \approx \frac{8\cdot 30\cdot 10^{-40}}{10^8\cdot 3\cdot 6{,}6^2\cdot 10^{-54}} \approx 2\cdot 10^6 \qquad (14.77)$$

and for the coefficient of absorption (14.74), assuming $\frac{\nu}{c} = \frac{10^{10}}{3\cdot 10^{10}} = \frac{1}{3}$, $\frac{h\nu}{kT} \approx \frac{1/3\ cm^{-1}}{200\ cm^{-1}} \approx 1{,}6\cdot 10^{-3}$ at $T = 300°$ (cf. (5.31)), we find that

$$\varkappa_\nu \approx \frac{1}{3}\cdot 6{,}6\cdot 10^{-27} n_m \cdot 1{,}6\cdot 10^{-3}\cdot 2\cdot 10^6 \approx 10^{-23} n_m. \qquad (14.78)$$

Taking into account n_m as equal to the number of particles per unit volume for a condensed medium on the order of 10^{22} cm^{-3}, we obtain $\varkappa_\nu \approx 10^{-1}$, i.e., the coefficient of absorption has a fairly large value. With a reduction in line width this coefficient will increase correspondingly.

Introducing the cross-section σ for absorption according to formula $\varkappa = \sigma n_0$, where n_0 is the number of absorbing particles (cf. (5.86))*, we obtain a value of σ on the order of 10^{-23} cm^2.

Absorption in forms containing 10^{11} absorbing particles (262) may be discovered in the most sensitive modern apparatuses for study of paramagnetic resonance under favorable conditions.

The simplest case of paramagnetic absorption is obtained when the absorbing atoms have orbitan moment equal to zero and one electron with non-compensated spin, given a spin moment of $S = s = 1/2$. This case occurs for atoms or ions with one external s-electron (basic condition of $^2S_{1/2}$; cf. Figures 6.1 and 8.3-8.7). As in the case of magnetic resonance in atomic beams, the transitions $-1/2 \longrightarrow 1/2$ and $1/2 \longrightarrow -1/2$ occur in a magnetic field (absorption and forced emanation; cf. Figure 14.12). In distinction from magnetic resonance in atomic beams the intensity of a single line obtained is determined by the difference between absorption and forced emanation (and not their sum).

An analogous case is found in more complex atomic systems for free radicals (chemically unstable), formed as intermediate products in chemical reactions and having one electron with non-compensated spin. Ordinary chemically stable molecules, as a rule, have an even number of electrons forming a saturated molecular envelope, and have complete mechanical and magnetic moments, equal to zero. In distinction from them, free radicals have a complete electronic mechanical moment $J = s = 1/2$, and correspondingly a complete magnetic moment $\mu_s = \mu_B$ (cf. (2.56)), and these radicals may be discovered easily, if their concentration is very low, by the paramagnetic resonance method (101).

---

*) If for the absorbing particles there is one basic level of the multiple $e_J = 2J + 1$, then at $\frac{\Delta E}{kT} \ll 1$ the constant A in (14.73) is equal to $\frac{1}{g_J}$ and $n_m \approx \frac{n_0}{g_J} = \frac{n_0}{2J+1}$, i.e., n_m and n_0 are of a single order.

For the case of atoms having electronic moment different from zero in their basic status and not having purely spin moment, a substantial difference is obtained upon investigation of magnetic resonance in atomic beams and in investigation of paramagnetic resonance. Because paramagnetic resonance usually is studied for substances in a condensed state, the absorbing atoms may not be considered free, as in the case of magnetic resonance in atomic beams. Even if the atom is not included in a molecule (which specifically occurs for paramagnetic ions in crystals) its main level splits in an electric field, formed by the surrounding particles, and the Zeeman split will be different from that obtained for a free atom*. Consideration of the problem of paramagnetic resonance in similar cases requires preliminary consideration of the interaction of the absorbing particles with the surrounding particles. The interaction between particles has a telling effect also on the contour of the paramagnetic resonance line. At the present time paramagnetic resonance is one of the effective methods for studying interaction between particles in a condensed system, and in general the structure of these systems both in solid and liquid state.

Magnetic resonant absorption by electrons of conductivity ("free electrons") which has been observed for metals constitutes a special case of paramagnetic resonance, and is due to their spin (259). The magnitude of splitting, as in the case of the $ns^2S_{1/2}$ status of atoms, is equal to $2\mu_B H$. Because penetration of a magnetic field into the metal is determined by the skin effect, diffusion of electrons in the range of the skin effect and outside this range plays an important role; this diffusion may be considered theoretical.

The ferromagnetic resonance (cf. page 2) observed in ferromagnetic bodies is a particular case of electronic spin magnetic resonance. It is connected with the spin interaction of particles in ferromagnetic bodies and is of interest from the point of view of the study of these interactions.

To the present we have discussed magnetic resonance caused by the presence of a constant magnetic moment in particles, which is oriented in the magnetic field, and which also causes the observed splitting of levels. For free electrons magnetic resonance caused by their movement in a magnetic field in a circular trajectory, or

---

*) This split does not occur in the case discussed above for atoms or ions in the basic state $^2S_{1/2}$ as a result of the theorem of Kramers; cf. Chapter 15.1, (205).

orbital movement, is possible. This type of resonance, connected with diamagnetism of free electrons, is called cyclotron resonance.

As is well known, an electron moving with speed v in a magnetic field describes a path like that of any charged particle*. The radius r of this trajectory (Figure 14.16) is determined by the $m_e \frac{v^2}{r}$ equilibrium condition of the centripetal force on the order of $\frac{evH}{c}$ of Lorentz $-\frac{e}{c}[vH]$, i.e., the condition $m_e \frac{v^2}{r} = \frac{e}{c} vH$. Thus the speed of motion in the circular trajectory is $\omega = \frac{v}{r} = \frac{eH}{m_e c}$ and the corresponding velocity is (cf. (2.46)

$$\nu = \frac{\omega}{2\pi} = \frac{eH}{2\pi m_e c} = \frac{2\mu_B H}{h}. \qquad (14.79)$$

The motion in the plane xy, perpendicular to the magnetic field, may be analyzed into two linear harmonic vibratory motions on the axes x and y, the quantizing of which gives the following possible energy values (cf. (145 and 146)):

$$E_n = h\nu\left(n + \frac{1}{2}\right) = \frac{ehH}{2\pi m_e c}\left(n + \frac{1}{2}\right) = \\ = 2\mu_B H\left(n + \frac{1}{2}\right) \quad (n = 0, 1, 2, \ldots). \qquad (14.80)$$

Thus instead of continuous levels of free electrons, discrete levels are obtained, the distance between which is equal to $2\mu_B H$ (Figure 14.17). The presence of similar quantizing leads to diamagnetism of free electrons.

This type of diamagnetism usually is called the diamagnetism of Landau; in 1930 Landau demonstrated experimentally (204) that according to the quantum theory free electrons have diamagnetism in distinction from the classic theory, in which diamagnetism of free electrons is lacking.

---

*) In particular, as in the case of charged heavy particles in a cyclotron, whence the name cyclotron resonance.

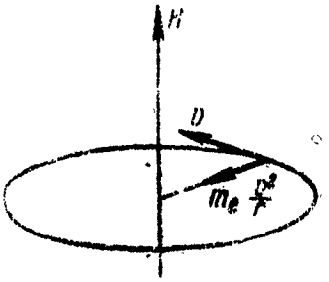

Figure 14.16. Movement of an electron in a circular trajectory.

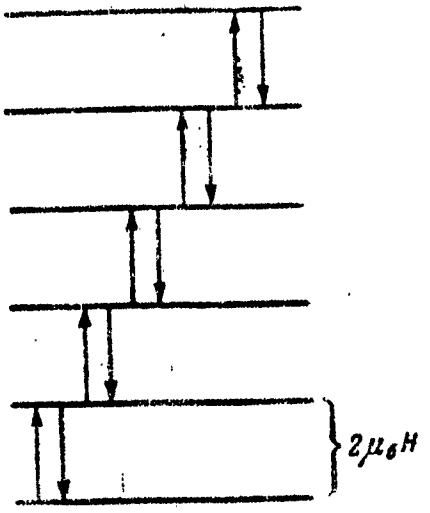

Figure 14.17. Energy levels for free electrons in a magnetic field.

Transitions are possible between levels of free electrons in a magnetic field through change of the quantum number n of the oscillator by ± 1. This is ordinary electric dipolar transition, corresponding to the components of dipolar moment perpendicular to the field, and consequently occurring under the effect of an alternating electric field of frequency ν, perpendicular to the permanent magnetic field. Forced transitions of this type (cyclotron resonance) are obtained when the frequency of the radio-frequency electric field perpendicular to the permanent magnetic field coincides with the frequency of transition.

From the classic point of view we have irradiation of frequency ν, determined by formula (14.79) and equal to $\frac{eH}{2\pi m_e c}$. In a coordinate system rotating with angular velocity $\omega = 2\pi\nu = \frac{eH}{m_e c}$, equal to twice the angular velocity (2.69) of Larmor precession, the electron will recede, and the magnetic field H cannot act on it. Thus precession occurs for free electrons in a magnetic field, the frequency of which is equal to twice the frequency of Larmor precession.

Cyclotron resonance is observed for slow electrons in the microwave range of the spectrum. Its measurement enables determination of the cyclotronic frequency (14.79). In the given magnetic field the ratio of the frequency of magnetic resonance for the investigated magnetic moment, proportionate to the magnitude μ of this moment (cf. (2.59)), may the cyclotron frequency may be measured, which is expressed by the Bohr magneton μ_B, or in other words, from the point of graphic representations, the ratio of the frequency of precession of the investigated magnetic moment to the frequency of precession of free electrons may be measured. In this, the value of magnetic moment is obtained directly in Bohr magnetons μ_B. The magnetic moment of the proton was measured with great precision by a similar method (268).

The anomaly of the magnetic moment of the electron was measured very precisely for free electrons through the difference between the frequency of precession of spin of the electron and the frequency of the cyclotronic resonance (at $g = 2$ these frequencies coincide and are equal to (14.79)). The measurements were performed with double dispersion (on gold foil) of an electron beam in a magnetic field, and gave the value (268).

$$\frac{g}{2} = \frac{\mu_{el}}{\mu_B} = (1{,}0011609 \pm 0{,}0000024), \qquad (14.81)$$

which is in complete agreement with (14.68).

According to the concept of Dorfman (260) the cyclotronic resonance may be obtained for conductive electrons in metals and semiconductors. In this, the actual electron mass m_e is replaced by the effective mass m_e^* in formula (14.79), the distance between levels in magnetic field is decreased by the function $\frac{m_e^*}{m_e}$ and the value of the effective mass may be determined according to the frequency of resonance. The cyclotronic resonance may be observed for semiconductors (silicon and germanium crystals) not only for electrons, but for gaps, as well (261).

BIBLIOGRAPHY

13. H. White, Introduction to Atomic Spectra, 1934.

14. Ye. Kondon and G. Shortli, "Theory of Atomic Spectra," IL, 1949.

17. E. Back and A. Landé, Zeeman-Effekt und Multiplettstruktur der der Spektrallinien, 1925;
E. Back, "Zeeman Effect," Handb. d. Phys., Vol. 22, p 1, 1929;
J. Van der Bosch, "Zeeman Effect," Handb. d. Phys., Vol 28, p. 296, 1957.

36. V. Ye. Arkad'yev, "On Magnetic Spectroscopy and Radio Spectroscopy of the Atomic Nucleus," UFN, Vol 44, p 60, 1951.

40. D. Ingram, "Spectroscopy at High and Ultra High Frequencies," IL, 1959.

41. M. A. Yel'yashevich, "Contemporary Status of Radio Spectroscopy," UFN, Vol 54, p 513, 1954.

42. N. Ramsey, "Molecular Beams," IL, 1960.

43. P. Kusch, "Atomic and Molecular Beam Spectroscopy," Handb. d. Phys., Vol 37/1, page 1, 1959.

101. D. Ingram, "Paramagnetic Resonance and Its Application to the Investigation of Free Radicals," IL, 1961

138. E. Wigner, Gruppentheorie und ihre Anwendunge auf die Quantenmechanik und Atomspektren, 1931.

145. S. V. Vonsovskiy, Sovremennoye ucheniye o magnetizme (Contemporary Views of Magnetism), State Publishing House for Technical Literature, 1952.

146. Ya. G. Dorfman, Magnitnye svoystve i stroyeniye veshchestva (Magnetic Properties and Structure of Matter) State Publishing House of Technical Literature, 1955.

203. J. Neumann and E. Wigner, Phys. Zs., Vols. 39, 467, 1929 (rule of non-intersection).

204. L. Landau, Zs. f. Phys., Vol 64, p 629, 1930 (diamagnetism of free electrons).

205. H. Kramers, Proc. Akad. Sci. Amst., Vol 33, p 959, 1930 (double degeneration in an electric field with an uneven number of electrons).

236. L. Ornstein and H. Burger, Zs. f. Phys., Vol 28, p 135, 1926; Vol 29, p 241, 1924;
R. Kronig and S. Goudsmit, Naturwiss., Vol 13, p 90, 1925; Zs. f. Phys., Vol 31, p 885, 1925;
H. Honl, Zs. f. Phys., Vol 31, p 340, 1925 (intensity of components in the Zeeman effect)

237. W. Pauli, Zs. f. Phys., Vol 16, p 155, 1923 (rule of sums for the g factor)

238. A. Shenstone and H. Blair, Phil. Mag., Vol 8, 765, 1925;
F. M. Gerasimov, ZHETF, Vol 9, p 1036, 1939 (analysis of incompleteness of resolution of the splitting picture in the Zeeman effect)

240. G. Harrison and F. Bitter, Phys. Rev., Vol 57, p 15, 1940 (the Zeeman effect in very strong magnetic fields)

241. L. D. Landau and Ye. M. Lifshits, Phys. Zs. d. Sow., Vol 8, p 1953, 1935 (Theory of ferromagnetic resonance)

242. B. G. Lazarev and L. V. Shubnikov, Phys. Zs. d. Sow., Vol 11, p 445, 1937 (discovery of nuclear paramagnetism)

243. I. Rabi, L. Zacharias, S. Milman and P. Kusch, Phys.Rev., Vol 53, p 318, 1938; Vol 55, 526, 1939;
I. Rabi, J. Zacharias, S. Milman and J. Kellog, Phys. Rev., Vol 55, p 728, 1939; Vol 56, p 728, 1939 (magnetic resonance in molecular beams)

244. P. Kusch, S. Milman and I. Rabi, Phys. Rev., Vol 57, p 765, 1940 (magnetic resonance in atomic beams).

245. Ye. K. Zavoyskiy, J. Phys. USSR, Vol 9, p 245, 1945; Vol 10, p 170, 1946 (discovery of paramagnetic resonance).

246. E. Purcell, H. Torrey and R. Pound, Phys. Rev., Vol 69, p 37, 1946;
F. Bloch, Phys. Rev., Vol 69, p 127, 1946; Vol 70, p 460, p 474, 1946 (discovery of nuclear magnetic resonance).

254. S. Koenig, A. Prodell and P. Kusch, Phys. Rev., Vol 83, p 687, 1951; Vol 88, p 191, 1952 (measurement of anomaly of the magnetic moment of the electron)

254 W. Nierenberg, Proc. Nat. Acad. Sci., Vol 45, p 429, 1959 (determination of the basic status of radioactive atoms in atomic beams)

254 C. Sommerfield, Phys. Rev., Vol 107, p 328, 1957 (computation of the anomaly of the magnetic moment of the electron).

259 F. Dyson, Phys. Rev., Vol 98, p 349, 1955 (electronic spin resonance absorption in metals)

260 Ya. G. Dorfman, DAN SSSR, Vol 81, p 765, 1951 (cyclotronic resonance of electrons of conductivity)

261 G. Dresselhaus, A. Kip and C. Kittel, Phys. Rev., Vol 98, p 368, 1955 (cyclotronic resonance for semiconductors).

262 H. Buckmaster and H. Scovil, Can. J. of Phys., Vol 34, p 711, 1956 (high sensitivity apparatus for investigation of paramagnetic resonance).

268 J. Gardner and E. Purcell, Phys. Rev., Vol 76, p 1262, 1949;
J. Gardner, Phys. Rev., Vol 83, p 996, 1951;
P. Franken and S. Liebes, Phys. Rev., Vol 104, p 1197, 1956 (measurement of the magnetic moment of the proton in Bohr magnetons)

318 D. Dennison, Rev. Mod. Phys., Vol 3, p 280, 1931 (part I); Vol 12, p 175, 1940 (Part II) (infrared spectra of simplest monatomic molecules).

- END -

520

CS/ 8324-D